Experimental Neurology 219 (2009) 104–111

Contents lists available at ScienceDirect

Experimental Neurology

journal homepage: www.elsevier.com/locate/yexnr

Neuronal differentiation of neural precursor cells is promoted by the methyl-CpG-binding protein MeCP2

Keita Tsujimura, Masahiko Abematsu, Jun Kohyama, Masakazu Namihira, Kinichi Nakashima *

Laboratory of Molecular Neuroscience, Graduate School of Biological Sciences, Nara Institute of Science and Technology, 8916-5, Takayama, Ikoma, Nara 630-0101, Japan

ARTICLE INFO

Article history:
Received 27 December 2008
Revised 2 April 2009
Accepted 2 May 2009
Available online 8 May 2009

Keywords:
MeCP2
Rett syndrome
Epigenetics
Differentiation
Neural stem cells
Cytokine
Transplantation

ABSTRACT

Methyl-CpG-binding protein 2 (MeCP2), a methyl-CpG-binding domain protein family member which is expressed predominantly in neurons in the nervous system, acts as a transcriptional repressor by binding to methylated genes, and mutations in *mecp2* cause the neurological disorder known as Rett syndrome (RTT). Although MeCP2 has been reported to regulate neuronal maturation rather than fate specification of neural precursor cells (NPCs), we have previously shown that it inhibits astrocyte differentiation of NPCs when ectopically expressed. Here, we show that expression of MeCP2 in NPCs not only suppresses astrocytic differentiation but actually promotes neuronal differentiation, even in the presence of well-known astrocyte-inducing cytokines. This dual function of MeCP2 was abolished by the MEK inhibitor U0126. Moreover, we observed that a truncated form of MeCP2 found in RTT patients fails to promote neuronal differentiation. We further demonstrate that transplanted MeCP2-expressing NPCs differentiate *in vivo* into neurons in two non-neurogenic regions, striatum and spinal cord. These results suggest a possible therapeutic application for MeCP2 in neurodegenerative diseases and injuries to the central nervous system.

Introduction

Neural stem and precursor cells (NSCs/NPCs) are defined as cells that can self-renew and can give rise to the three major cell types in the nervous system: neurons, astrocytes, and oligodendrocytes (Gage, 2000). Specification of NSC/NPC lineages is regulated by cell-external cues and cell-intrinsic programs (Edlund and Jessell, 1999; Hsieh and Gage, 2004).

Cell-external cues include various types of cytokines whose signals are transduced into the nucleus with the mediation of transcription factors. Leukemia inhibitory factor (LIF), a member of the interleukin-6 (IL-6) family of cytokines that share gp130 as a signal-transducing receptor component, can effectively induce astrocyte differentiation via the Janus kinase (JAK)-signal transducer and activator of transcription (STAT) signaling pathway (Bonni et al., 1997; Nakashima et al., 1999a,b; Rajan and McKay, 1998). Bone morphogenetic proteins (BMPs), which belong to the transforming growth factor β superfamily, also induce astrocytic differentiation of NPCs (Gomes et al., 2003; Gross et al., 1996; Nakashima et al., 2001).

Cell-intrinsic programs involve epigenetic changes such as DNA methylation and histone modifications. DNA methylation at the dinucleotide CpG is one of the best-studied epigenetic modifications in multicellular genomes (Bird, 2002). NPCs at midgestation differentiate only into neurons and not into astrocytes (Qian et al., 2000), even when stimulated by LIF, due to DNA hyper-methylation in the promoter regions of astrocyte-specific genes such as glial fibrillary acidic protein (*gfap*) (Fan et al., 2005; Namihira et al., 2004; Takizawa et al., 2001). As gestation proceeds, these promoters become demethylated, enabling NPCs to differentiate into astrocytes at a later stage of development. Although late-gestational NPCs, whose astrocytic gene promoters have already become demethylated, can still give rise to neurons, these neurons do not respond to astrocyte-inducing cytokines to express *gfap* (Kohyama et al., 2008; Setoguchi et al., 2006).

Methyl-CpG-binding protein 2 (MeCP2) belongs to the methyl-CpG-binding domain (MBD) protein family, whose members function as transcriptional repressors by binding to methylated DNA (Klose and Bird, 2006; Meehan et al., 1992). MeCP2 binds to a single symmetrically methylated CpG dinucleotide via its MBD, and silences genes via its transcriptional repression domain (TRD) (Jones et al., 1998; Nan et al., 1998). MBD proteins including MeCP2 are expressed predominantly in neurons in the mammalian central nervous system (CNS) (Jung et al., 2002; Shahbazian et al., 2002). Mutations in *mecp2* cause Rett syndrome (RTT), a neurodevelopmental disorder characterized by mental retardation, motor dysfunction and autistic behavior. Recently, it was reported that MeCP2 is involved in neuronal maturation rather than cell fate decisions (Kishi and Macklis, 2004), although another study suggested that MeCP2 also plays a role in cell fate decisions during primary neurogenesis in *Xenopus* embryos by recruiting the transcription repressor complex (Stancheva et al., 2003).

* Corresponding author. Fax: +81 743 72 5479.
E-mail address: kin@bs.naist.jp (K. Nakashima).

0014-4886/$ – see front matter © 2009 Elsevier Inc. All rights reserved.
doi:10.1016/j.expneurol.2009.05.001

We have previously shown that MeCP2 prevents the conversion of neurons to astrocytes by binding to highly methylated regions encompassing the transcription initiation sites of astrocytic genes (Kohyama et al., 2008; Setoguchi et al., 2006). Here, we show that ectopic MeCP2 expression in late-gestational NPCs inhibits astrocytic differentiation and promotes neuronal differentiation, even in the presence of astrocyte-inducing cytokines. Inhibition of the Ras-extracellular signal-regulated kinase (ERK) pathway with a MEK inhibitor abolished these MeCP2 effects. A mutant form of MeCP2, R168X, which occurs with high incidence in RTT patients, could not promote neuronal differentiation of NPCs. We further demonstrate that MeCP2 can enhance neuronal differentiation of NPCs transplanted into non-neurogenic CNS tissue *in vivo*.

Experimental procedures

NPC culture

Time-pregnant ICR mice were used to prepare NPCs. The experimental protocols described below were performed according to the animal experimentation guidelines of Nara Institute of Science and Technology. NPCs were prepared from telencephalons of E14.5 mice and cultured as described previously (Nakashima et al., 1999a,b). Briefly, the telencephalons were triturated in Hank's balanced salt solution (HBSS) by mild pipetting with a 1-ml pipet tip (Gilson, Middleton, WI, USA). Dissociated cells were cultured for 4 days prior to each experiment in N2-supplemented Dulbecco's modified Eagle's medium with F12 (Gibco, Grand Island, NY, USA) containing 10 ng/ml basic fibroblast growth factor (bFGF; R and D Systems, Minneapolis, MN, USA; N2/DMEM/F12/bFGF) on culture dishes (Nunc, Naperville, IL, USA) or chamber slides (Nunc) that had been precoated with poly-L-ornithine (Sigma, St. Louis, MO, USA) and fibronectin (Sigma).

Inhibitor experiment

U0126 (Calbiochem, Darmstadt, Germany) was dissolved in dimethyl sulfoxide (DMSO) at 10 mM, and stored at −20 °C. At the time of treatment, stocks of the inhibitor were thawed, prediluted in medium, and then added to the well up to 8 μM.

Immunocytochemistry

Cells cultured on coated chamber slides were washed with phosphate-buffered saline (PBS), fixed in 4% paraformaldehyde in PBS, and stained with combinations of the following primary antibodies: chick anti-green fluorescent protein (GFP) (1:1000; Aves Labs, Tigard, OR, USA), rabbit anti-GFP (1:1000; MBL, Nagoya, Japan), rabbit anti-βIII-tubulin (Tuj1; 1:1000; Covance, Berkeley, CA, USA), mouse anti-microtubule-associated proteins 2a and 2b (MAP2ab; 1:250; Sigma), guinea pig anti-GFAP (1:2500; Advanced Immunochemical, Long Beach, CA, USA), goat anti-doublecortin (DCX) (1:1000; Santa Cruz Biotechnology, Santa Cruz, CA, USA), mouse anti-S100β (1:1000; Sigma), rabbit anti-aquaporin 4 (AQP4) (1:500; Santa Cruz), chick anti-myelin basic protein (MBP) (1:200; Aves Labs), mouse anti-Nestin (1:1000; Chemicon, Temecula, CA, USA), rabbit anti-cleaved-caspase3 (1:1000; Cell Signaling, Danvers, MA, USA), and mouse anti-Ki67 (1:1000; BD, Franklin Lakes, NJ, USA). The following secondary antibodies were used: FITC-conjugated donkey anti-chick IgY (1:500; Jackson ImmunoResearch, West Grove, PA, USA), Cy3-conjugated donkey anti-mouse IgG (1:500; Chemicon), Cy3-conjugated donkey anti-rabbit IgG (1:500; Jackson ImmunoResearch), Alexa488-conjugated donkey anti-rabbit (1:500; Molecular Probes, Eugene, OR, USA), and Cy5-conjugated donkey anti-guinea pig (1:500; Jackson ImmunoResearch). Nuclei were stained using bisbenzimide H33258 fluorochrome trihydrochloride (Nacalai Tesque, Kyoto, Japan).

Immunohistochemistry

Brains and spinal cords from mice transcardially perfused with PBS followed by 4% paraformaldehyde were dissected, post-fixed overnight at 4 °C, and then transferred to 20% sucrose in PBS for 24 h at 4 °C. Brains and spinal cords were sectioned at 40 μm with a cryostat (Leica, Tokyo, Japan). Sections were stained with combinations of the following primary antibodies: rabbit anti-GFP (1:1000; MBL, Nagoya, Japan), goat anti-DCX (1:1000; Santa Cruz), and guinea pig anti-GFAP (1:2500; Advanced Immunochemical). The following secondary antibodies were used: Cy3-conjugated donkey anti-goat IgG (1:500; Jackson ImmunoResearch), Alexa488-conjugated donkey anti-rabbit (1:500; Molecular Probes), and Cy5-conjugated donkey anti-guinea pig (1:500; Chemicon). Nuclei were stained using bisbenzimide H33258 fluorochrome trihydrochloride (Nacalai Tesque).

Recombinant retrovirus construction and infection

Rat *mecp2* and *mecp2* (R168X) cDNAs were cloned into the expression vector pMY containing an internal ribosome entry site upstream of the GFP gene (Morita et al., 2000). The Plat-E packaging cell line was transiently transfected with these constructs using Trans-IT 293 (Mirus, Madison, WI, USA) (Morita et al., 2000). On the following day, the medium was replaced with N2/DMEM/F12/bFGF, and the cells were cultured in this medium for 1 day before virus was collected.

Transplantation into striatum

Adult ICR mice were anesthetized by intraperitoneal injection of ketamine (100 mg/kg) and xylazine (10 mg/kg). Mice were stereotaxically injected, with 2 μl of N2-supplemented DMEM/F12 medium containing 10^6 NPCs infected with retroviruses expressing GFP or GFP together with MeCP2, into the striatum (coordinates from bregma were 0 mm posterior, 2 mm lateral and 2.9 mm deep from the brain surface) using a stereotaxic apparatus (Narishige, Tokyo, Japan).

Transplantation into spinal cord

Adult ICR mice were anesthetized as above. After laminectomy at the ninth and tenth thoracic spinal vertebrae, we exposed the dorsal surface of the dura mater. Two μl of N2-supplemented DMEM/F12 medium containing 10^6 NPCs was transplanted into the spinal cord using a microinjector (Narishige).

Results

MeCP2 promotes neuronal differentiation even in the presence of astrocyte-inducing cytokines

We have previously shown that ectopic expression of MeCP2 in NPCs suppresses astrocytic differentiation induced by LIF (Kohyama et al., 2008; Setoguchi et al., 2006). In light of this finding, we anticipated that MeCP2 would also be able to influence neuronal differentiation of NPCs. To test this, we expressed GFP alone (control) and GFP together with MeCP2 by retroviral infection in E14.5 NPCs (Fig. 1A). We first examined the effect of MeCP2 in the absence of astrocyte-inducing cytokine. Ectopically expressed MeCP2 was able to enhance neuronal differentiation compared to the control during a 4-day culture after virus infection (Figs. 1B and C). The percentages of cells positive for markers of astrocytes (GFAP), oligodendrocytes (MBP) and undifferentiated NSCs/NPCs (Nestin) among GFP-positive cells were similar between control and MeCP2-expressing virus-infected cells (Figs. 1B, C and Supplemental Fig 1B). When we extended the culture period after virus infection to 8 days, the percentage of Nestin-positive cells among GFP-positive cells decreased to 10–20% in both control and

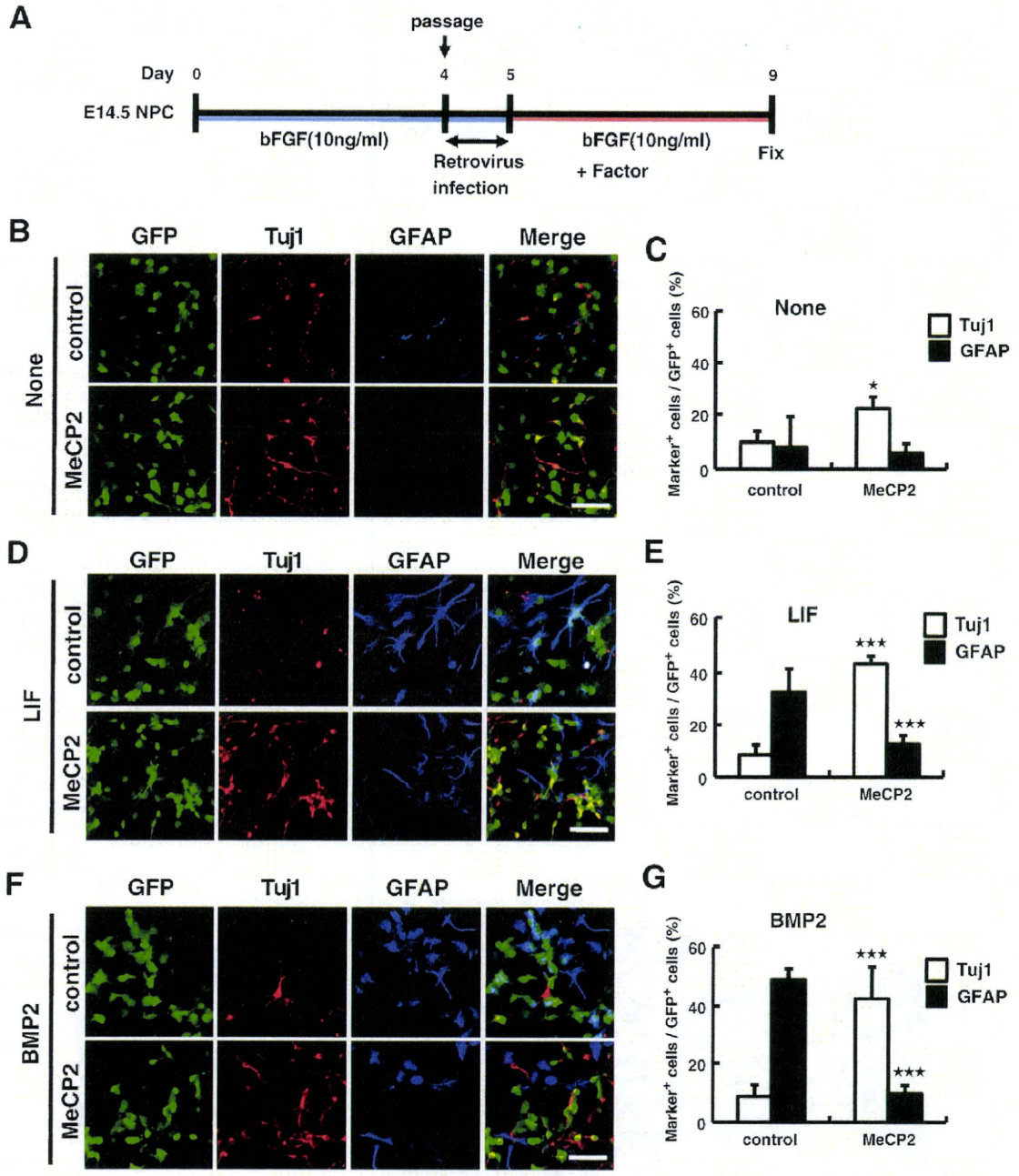

Fig. 1. MeCP2 promotes neurogenesis even in the presence of astrocyte-inducing cytokines. (A) Schematic of the cell culture and virus infection time course. (B, D and F) NPCs infected with recombinant retroviruses engineered to express only GFP (upper panels) or MeCP2 together with GFP (lower panels) were cultured for 4 days in the presence of bFGF (1 ng/ml) alone (B) or together with either LIF (50 ng/ml) (D) or BMP2 (50 ng/ml) (F). The cells were then stained with antibody for GFP (green), βIII-tubulin (Tuj1, red) and GFAP (blue). Scale bar = 50 μm. (C, E and G) Tuj1- and GFAP-positive cells in GFP-positive cells in (B), (D) and (F) were quantified (mean ± S.D.; *t*-test, $^{*}P<0.05$ and $^{***}P<0.001$ compared with the control).

MeCP2-expressing cells, suggesting that the NPC population had matured compared to the 4-day culture (Supplemental Fig. 1C). Even in this prolonged culture, MeCP2 expression still promoted neuronal differentiation of NPCs compared to control (Supplemental Fig. 1C).

To examine whether MeCP2 can induce neuronal differentiation even in the presence of astrocyte-inducing factors, virus-infected NPCs were cultured with LIF or BMP2. As we have shown previously, MeCP2 expression inhibited cytokine-induced astrocytic differentiation of NPCs. Surprisingly, MeCP2 could promote neuronal differentiation more effectively in the presence of LIF than in its absence (Figs. 1D and E). This effect of MeCP2 was also observed with BMP2 (Figs. 1F and G). Moreover, MeCP2 enhanced expression of another neuronal marker, MAP2ab, in the presence of either LIF or BMP2 (Supplemental Figs. 2A and B). We further examined whether MeCP2 suppresses other astrocytic markers in the presence of LIF, and found that MeCP2 indeed inhibited the expression of AQP4 and S100β (Supplemental Fig. 3).

We then asked whether this fate switch was due to increased proliferation and/or survival of NPCs expressing MeCP2. E14.5 NPCs were infected with retrovirus to express GFP either alone or together with MeCP2. Two days later, we assessed cell proliferation and survival by immunocytochemistry using antibodies against Ki-67 (a

proliferation marker) or cleaved-caspase3 (an apoptosis marker) (Supplemental Fig. 4). The expression of MeCP2 had no significant effect on either proliferation or apoptosis (Supplemental Figs. 4B and C).

Since NPCs in primary culture are known to be a heterogeneous population containing differentiated neural cells as well as multipotent and lineage-committed NPCs, we performed the same experiments as those in Fig. 1 using NSCs, which had been cultured under conditions that sustain pure symmetrical divisions of NSCs without accompanying differentiation (Conti et al., 2005; Pollard et al., 2006). As shown in Supplemental Fig. 5A, almost all of the cells were immunoreactive for the undifferentiated NSC/NPC markers Sox2 and Nestin; none was stained by antibodies for the differentiation markers Tuj1, GFAP and MBP. Even in this homogeneous population, MeCP2 expression enhanced neuronal differentiation to an extent comparable to that observed in the primary NPC culture (Supplemental Figs. 5B–F).

Collectively, these results indicate that MeCP2 not only suppresses astrocytic differentiation but also promotes neuronal differentiation of multipotent NSCs/NPCs in the presence of astrocyte-inducing cytokines.

MeCP2 expression does not affect methylation status of the gfap promoter

The expression of astrocytic genes is regulated decisively by their promoter methylation status during development (Namihira et al., 2004, 2009; Takizawa et al., 2001). We therefore examined the possibility that MeCP2 expression re-induces methylation in the *gfap* promoter. This, however, is not the case: the *gfap* promoter was maintained in a hypo-methylated state regardless of MeCP2 expression (Supplemental Fig. 6). Furthermore, we have previously shown that exon 1 of *gfap* is hyper-methylated even in NPCs which have already lost methylation in the *gfap* promoter, and that MeCP2 can bind to the hyper-methylated exon 1 to suppress *gfap* expression (Setoguchi et al., 2006; Kohyama et al., 2008). Sustained hyper-methylation of the *gfap* exon 1 in control and MeCP2-expressing virus-infected cells was also confirmed in the present study, suggesting that MeCP2 binds this region to inhibit astrocytic gene expression.

Inhibition of the Ras-ERK pathway abolishes MeCP2-mediated neuronal differentiation

It has been suggested that activation of the Ras-ERK pathway is important for neuronal differentiation (Menard et al., 2002; Paquin et al., 2005). The culture medium used in our experiments contains insulin and bFGF, which activate the Ras-ERK pathway (Avruch, 1998; Kouhara et al., 1997). Therefore, we examined whether the anti-gliogenic and pro-neurogenic functions of MeCP2 require activation of the Ras-ERK pathway, using U0126, an inhibitor of the ERK-upstream kinase MEK. NPCs were infected with control and MeCP2-expressing retroviruses and cultured with or without U0126 in the presence of bFGF (1 ng/ml) and LIF (50 ng/ml). MeCP2-expressing NPCs differentiated into Tuj1-positive neurons without U0126 as in Fig. 1, but in the presence of U0126 these cells differentiated into GFAP-positive astrocytes at the expense of Tuj1-positive neurons (Figs. 2A and B). In contrast, treatment with U0126 did not affect differentiation of control virus-infected NPCs. Similar results were also obtained in the case of BMP2 stimulation (Figs. 2A and C). Taken together, these observations suggest that the Ras-ERK pathway plays a critical role in MeCP2-mediated regulation of NPC fate specification.

A mutant form of MeCP2 can neither promote neuronal differentiation nor suppress astrocytic differentiation

Mutations in *mecp2* cause RTT (Amir et al., 1999). To determine whether a representative mutant form of MeCP2 that is found in

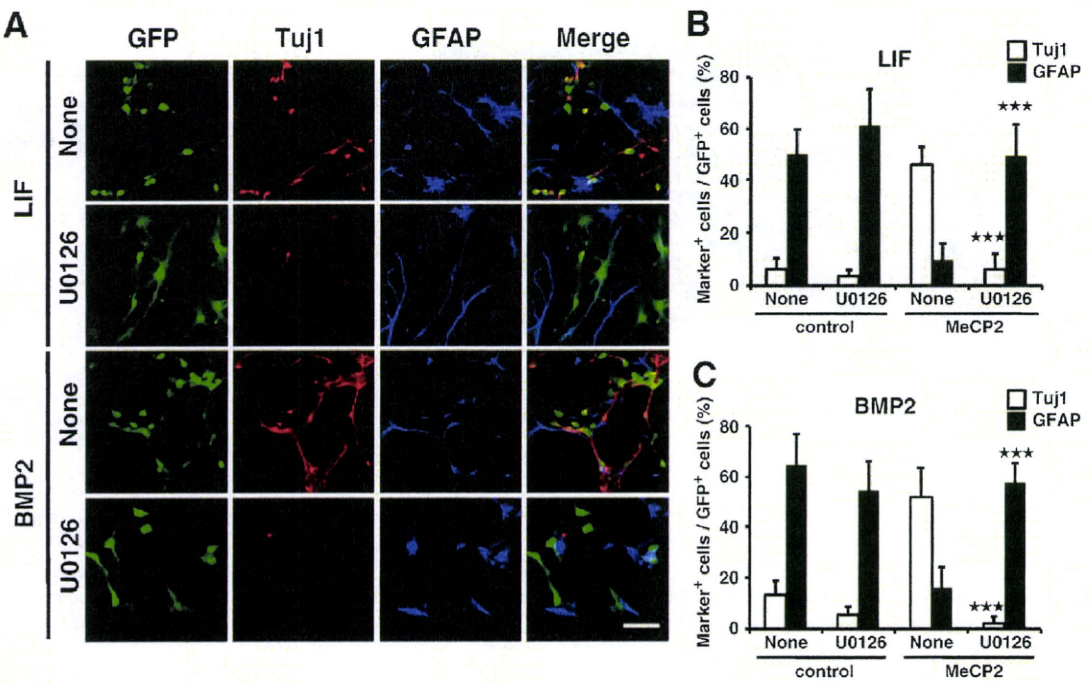

Fig. 2. Inhibition of the Ras-ERK pathway abolishes neuronal differentiation mediated by MeCP2. (A) NPCs infected with recombinant retroviruses engineered to express only GFP (not shown) or MeCP2 together with GFP were cultured with (second and bottom rows) or without (top and third rows) the MEK inhibitor U0126 (8 μM) for 4 days in the presence of bFGF (1 ng/ml) together with either LIF (50 ng/ml) or BMP2 (50 ng/ml). The cells were then stained with antibody for GFP (green), βIII-tubulin (Tuj1, red) and GFAP (blue). Scale bar = 50 μm. (B and C) Tuj1- and GFAP-positive cells in GFP-positive cells cultured as in (A) were quantified (mean ± S.D.; *t*-test, ***$P<0.001$ compared with the control).

RTT patients also exerts the dual function of wild type MeCP2 described above, i.e., inhibition of glial differentiation and promotion of neuronal differentiation, we used R168X, a truncated mutant form of MeCP2 which is observed at high frequency in classic RTT (Amir and Zoghbi, 2000) and lacks the C-terminal two-thirds of the polypeptide including the TRD (Fig. 3A). NPCs were infected with full-length MeCP2- or R168X-expressing retroviruses and cultured in the presence of LIF for 4 days. In contrast to the behavior of intact MeCP2, R168X was unable either to enhance neuronal differentiation or to suppress astrocytic differentiation (Figs. 3B and C). This loss of wild type MeCP2 function was also displayed by R168X in the presence of BMP2 (Figs. 3D and E). These results indicate that the TRD and C-terminal region are required for the dual function of MeCP2.

MeCP2 enhances neuronal differentiation of NPCs in non-neurogenic regions in vivo

BMP2 and/or BMP4 are physiologically expressed in the striatum, a non-neurogenic region in the adult brain, where they inhibit neurogenesis (Gross et al., 1996; Lim et al., 2000). Given that MeCP2 promotes neuronal differentiation even in the presence of BMP2 in *in vitro* experiments, we next asked whether MeCP2 can also enhance neuronal differentiation and suppress astrocytic differentiation in the striatum. We transplanted NPCs infected with retroviruses expressing GFP (control) or GFP together with MeCP2 into the striatum (Fig. 4A). One week after transplantation, more than half of the control NPCs had differentiated into GFAP-positive astrocytes (Figs. 4B and C). In marked contrast, NPCs expressing MeCP2 differentiated dramatically into DCX-positive immature neurons. Quantitative analysis revealed that 59% and only 11% of control NPCs became GFAP- and DCX-immunoreactive cells, respectively, whereas 10% and 62% of MeCP2-expressing NPCs became GFAP- and DCX-immunoreactive cells, respectively (Fig. 4C). This differentiation tendency was also observed at 2 weeks post-transplantation (Supplemental Fig. 7A). Thus, these results reveal that MeCP2 enhances neuronal differentiation and inhibits astrocytic differentiation in the striatum, a well-known non-neurogenic region.

A previous study has suggested that NPCs grafted into another non-neurogenic region, the spinal cord, were restricted to the glial

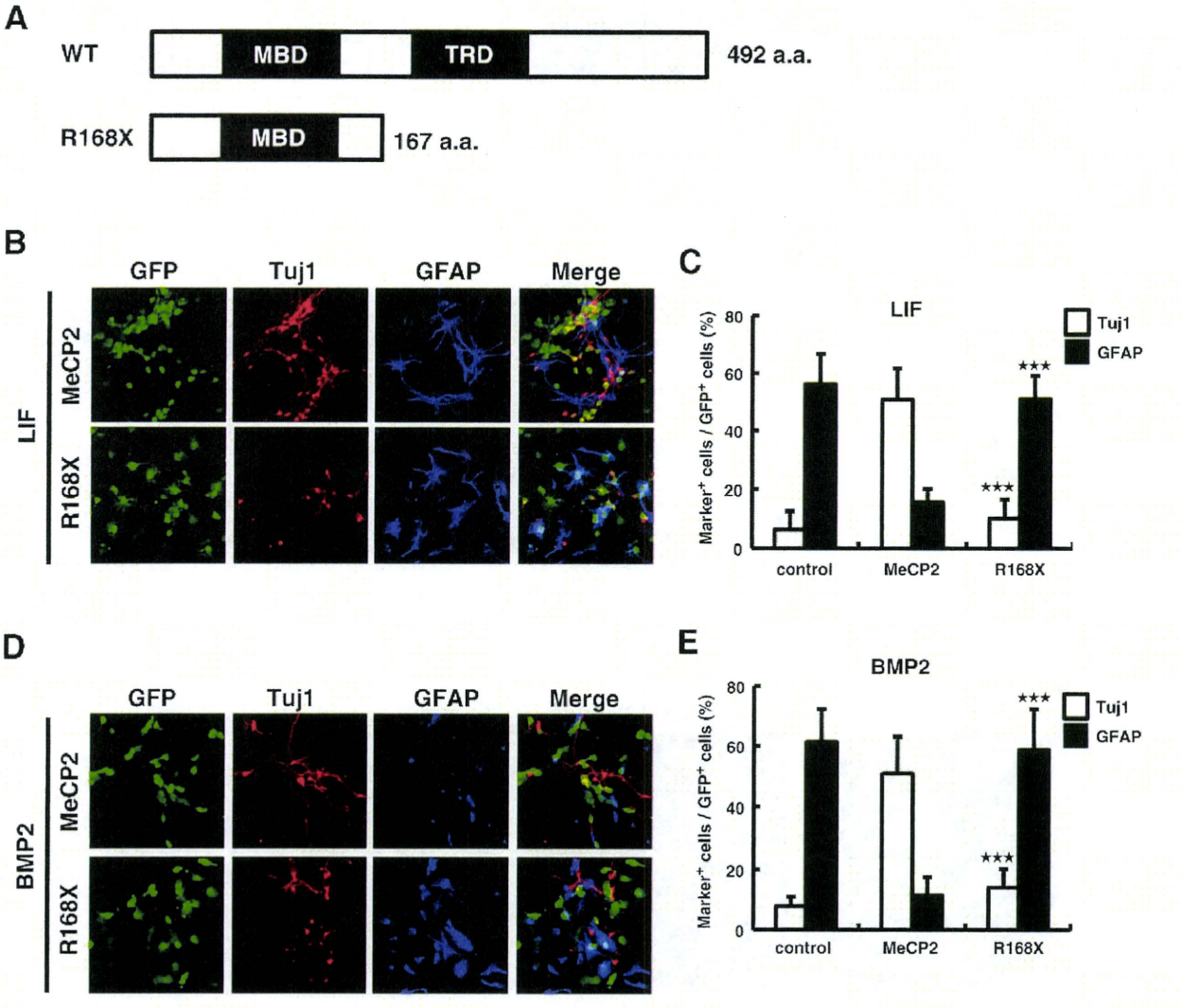

Fig. 3. A truncated form of MeCP2 found in RTT patients cannot promote neuronal differentiation. (A) Schematic illustration of full-length (WT) and a mutant form (R168X) of MeCP2. a.a., amino acids. (B and D) NPCs infected with recombinant retroviruses engineered to express MeCP2 together with GFP or R168X together with GFP were cultured for 4 days in the presence of bFGF (1 ng/ml) together with either LIF (50 ng/ml) (B) or BMP2 (50 ng/ml) (D). The cells were then stained with antibody for GFP (green), βIII-tubulin (Tuj1, red) and GFAP (blue). Scale bar = 50 μm. (C and E) Tuj1- and GFAP-positive cells in GFP-positive cells in (B) and (D) were quantified (mean ± S.D.; *t*-test, $^{***}P<0.001$ compared with WT MeCP2).

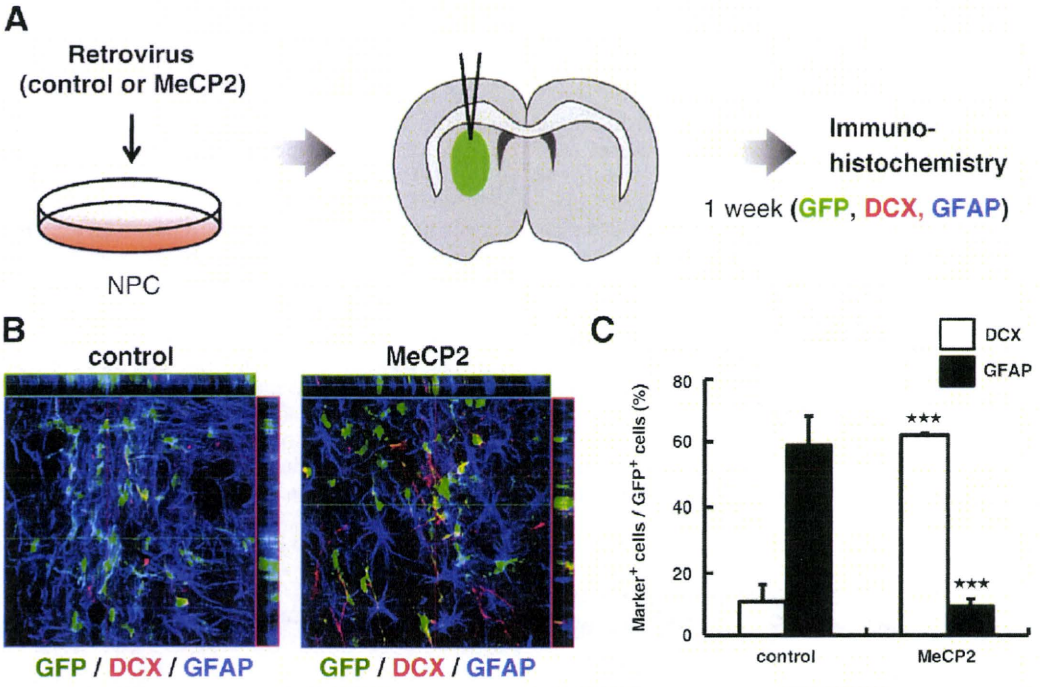

Fig. 4. MeCP2-expressing NPCs differentiate into neurons in the striatum. (A) Schematic of the experiment. The green oval indicates the cell-transplanted region in the striatum. (B) NPCs infected with recombinant retroviruses engineered to express only GFP or MeCP2 together with GFP were transplanted into the striatum. One week after transplantation, the mice were killed and brain tissue sections were stained with antibody for GFP (green), DCX (red) and GFAP (blue). Scale bar = 50 μm. (C) DCX- and GFAP-positive cells in GFP-positive cells in (B) were quantified (mean ± S.D.; *t*-test, $n = 3$; ***$P < 0.001$ compared with the control).

lineage (Cao et al., 2001). To investigate whether MeCP2 can also promote neuronal differentiation and inhibit astrocytic differentiation in this region, we transplanted NPCs infected with control and MeCP2-expressing retroviruses into spinal cord (Fig. 5A). One week after transplantation, we found that 56% of control NPCs had differentiated into GFAP-positive astrocytes and 9% into DCX-

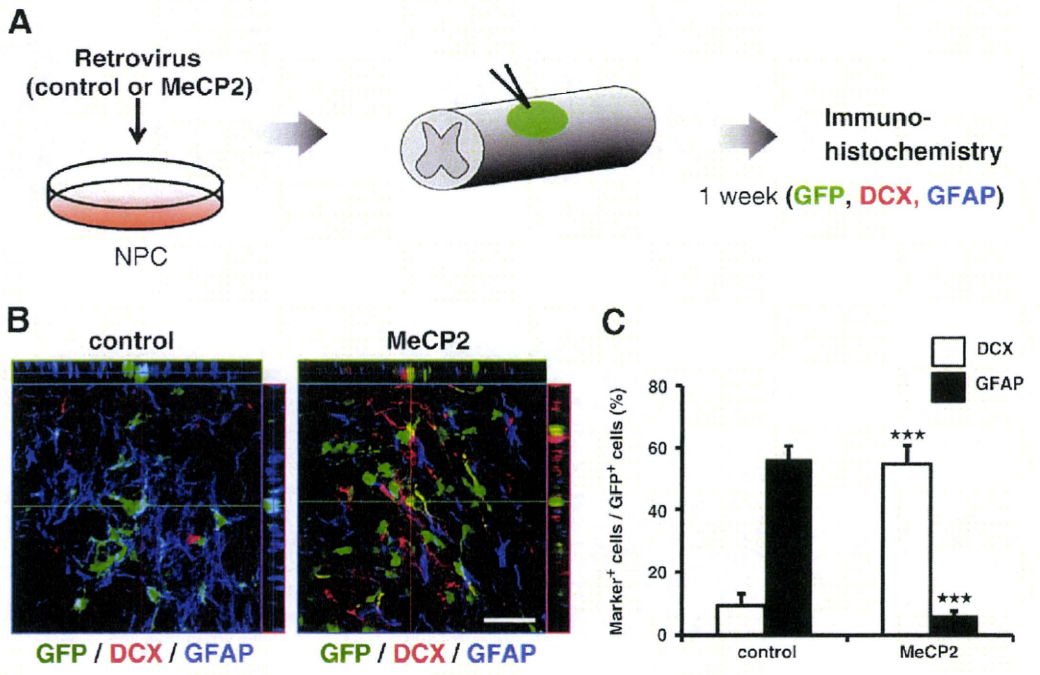

Fig. 5. MeCP2-expressing NPCs differentiate into neurons in the spinal cord. (A) Schematic of the experiment. The green oval indicates the cell-transplanted region in the spinal cord. (B) NPCs infected with recombinant retroviruses engineered to express only GFP or MeCP2 together with GFP were transplanted into the intact spinal cord. One week post-transplantation, the mice were killed and spinal cord tissue sections were stained with antibody for GFP (green), DCX (red) and GFAP (blue). Scale bar = 50 μm. (C) DCX- and GFAP-positive cells in GFP-positive cells in (B) were quantified (mean ± S.D.; *t*-test, $n = 3$; ***$P < 0.001$ compared with the control).

positive neurons. In contrast to the control NPCs, 54% of transplanted MeCP2-expressing NPCs differentiated into DCX-positive neurons and 6% into GFAP-positive astrocytes (Figs. 5B and C). These tendencies were also observed at 2 weeks post-transplantation (Supplemental Fig. 7B). MeCP2 therefore also enhances neuronal differentiation and inhibits astrocytic differentiation of NPCs in the non-neurogenic spinal cord.

Discussion

Mutations in *mecp2* cause Rett syndrome. MeCP2 is expressed predominantly in neurons in the CNS and functions as a repressor of gene transcription. However, the molecular mechanisms by which MeCP2 dysfunction leads to the neural-specific phenotypes of RTT remain poorly understood (Chen et al., 2001). Kishi and Macklis (2004) have reported that MeCP2 is involved in neuronal maturation rather than cell fate determination, as judged from both *in vivo* and *in vitro* analysis of MeCP2 mutant mice. In the present study, we have demonstrated that ectopic expression of MeCP2 in NPCs not only suppresses astrocytic differentiation but also promotes neuronal differentiation in both *in vitro* and *in vivo* conditions. These results clearly suggest that MeCP2 has the potential to regulate fate determination of NPCs under certain circumstances. We also showed that R168X, a truncated form of MeCP2 found in RTT patients, lacks the dual function of full-length MeCP2. This finding indicates that R168X is not functional and may partially explain RTT pathology. In support of this, it has been reported that transcription of several astrocytic genes, including *gfap*, is upregulated in RTT patients (Colantuoni et al., 2001).

The Ras-ERK pathway has been suggested to be important for neuronal differentiation of NPCs (Menard et al., 2002; Paquin et al., 2005). We demonstrated in this study that the MEK inhibitor U0126 abolished the capacity of MeCP2 to promote neuronal differentiation and to suppress astrocytic differentiation, suggesting that ERK activation is, at least in part, involved in the function of MeCP2. Thus, it is possible that MeCP2 is phosphorylated by ERK to form a functional complex with other relevant proteins. Regarding MeCP2 phosphorylation, it has been reported that MeCP2 is phosphorylated at serine 421 by a CaMKII-dependent mechanism in response to neuronal activity, and is also phosphorylated at serines 80 and 229 independently of neuronal activity (Zhou et al., 2006). In this context, we constructed three mutant forms of *mecp2*, each encoding a single serine-to-alanine mutation at position 80, 229 or 421. However, these mutants exerted the same dual function as was observed with intact MeCP2 (data not shown).

An important question still remains unsolved: how does MeCP2 respectively enhance and inhibit neuronal and astrocytic differentiation? One possibility is that MeCP2 represses the expression of repressors of neuronal differentiation such as neuron-restrictive silencer factor/RE-1 silencing transcription factor (NRSF/REST), which is a repressor of neuronal genes in non-neuronal cells (Chong et al., 1995; Schoenherr and Anderson, 1995). It has been suggested that neurogenin1 (NEUROG1), a proneural basic helix–loop–helix (bHLH) transcription factor, can inhibit transcription of *gfap* by sequestering the CREB binding protein (CBP)-Smad1 complex away from astrocyte-specific genes and by inhibiting the activation of STATs, which are necessary for astrocyte differentiation (Sun et al., 2001). Therefore, it is possible that expression of proneural bHLH genes such as *Neurog1* is somewhat induced, and that the gene product(s) function in concert with MeCP2. It has recently been suggested that MeCP2 associates with the transcriptional activator cAMP responsive element binding protein (CREB) and can thereby function as an activator of transcription (Chahrour et al., 2008). CREB was shown to be phosphorylated by ERK (Brami-Cherrier et al., 2005). Thus, it is likely that MeCP2 associates with phosphorylated CREB to function as a transcriptional activator, which may explain why the MEK inhibitor U0126 impeded MeCP2-mediated neuronal differentiation of NPCs. However, further investigation will be needed to precisely verify the mechanism whereby MeCP2 regulates differentiation of NPCs.

Since spontaneous recovery is very limited in the damaged mammalian CNS, NPCs are currently considered a promising cell source for cell replacement strategies aimed at treating neurodegenerative diseases and CNS injuries. Inflammatory cytokines, such as LIF and BMPs, which promote astrocytic differentiation are upregulated in lesion sites of the CNS (Nakamura et al., 2003; Setoguchi et al., 2004). Adult NPCs proliferate in response to injury, but the vast majority of newly generated cells differentiate into astrocytes (Johansson et al., 1999; Namiki and Tator, 1999), and this is also the case for exogenous NPCs that are transplanted into the injured CNS (Ogawa et al., 2002; Vroemen et al., 2003). This astrocytic differentiation of NPCs at the expense of neuronal differentiation is one of the major current obstacles in regeneration therapy. The gliogenic environment pertaining in the adult CNS is thought to be governed by extrinsic environmental factors, such as LIF and BMPs. Thus, tools that are capable of preventing astrocytic differentiation and stimulating other lineages in endogenous NSCs and grafted cells may be key factors for functional recovery. In this study, we have demonstrated that MeCP2 dramatically enhances neuronal differentiation and inhibits astrocytic differentiation even in the presence of astrocyte-inducing cytokines, both *in vitro* and in non-neurogenic striatum and spinal cord *in vivo*, raising the possibility that MeCP2 could be used to regulate NPC fate decision and thereby to improve functional recovery in the damaged CNS.

A previous study suggested that transduction of NPCs with *Neurog2* before transplantation inhibited astrocyte differentiation and improved functional recovery in the rat model of spinal cord injury (Hofstetter et al., 2005). However, the expression of *Neurog2* is transient during development, and is downregulated when neurons become mature. Therefore, continuous expression of *Neurog2* in engrafted cells might lead to unforeseen adverse side-effects. On the other hand, MeCP2 protein levels increase as neurons mature, and *mecp2* expression is sustained in mature neurons (Kishi and Macklis, 2004). We therefore anticipate that transduction of NPCs with *mecp2* would have fewer undesirable side-effects than that with *Neurog2*. However, it has also been reported that expression levels of MeCP2 are critical for normal neurological function (Chao et al., 2007), and that transgenic mice expressing excess *mecp2* display neurological dysfunction similar to that seen in RTT (Collins et al., 2004). To achieve optimal regulation of neuronal function, therefore, it may be necessary to control the MeCP2 expression level in NPCs.

In conclusion, our findings open a promising new avenue for promoting the ability of NPCs to generate the large numbers of neurons that will be required for restorative treatment of neurodegenerative disorders and injured nervous systems. Testing this possibility must await further investigation.

Acknowledgments

We thank Dr. T. Kitamura (Tokyo University) for pMY vector and Plat-E cells. We appreciate Drs. Y. Bessho and T. Matsui for valuable discussions. We also thank Dr. I. Smith for helpful comments and critical reading of the manuscript. We are very grateful to N. Ueda and M. Tano for excellent secretarial assistance. Many thanks to N. Namihira for technical help. This work has been supported by the Suzuken Memorial Foundation, the TERUMO Lifescience Foundation, the Mochida Memorial Foundation for Medical and Pharmaceutical Research, and by a Grant-in-Aid for Science Research on Priority Areas and the NAIST Global COE Program (Frontier biosciences: strategies for survival and adaptation in a changing global environment) from the Ministry of Education, Culture, Sports, Science and Technology of Japan.

Appendix A. Supplementary data

Supplementary data associated with this article can be found, in the online version, at doi:10.1016/j.expneurol.2009.05.001.

References

Amir, R.E., Zoghbi, H.Y., 2000. Rett syndrome: methyl-CpG-binding protein 2 mutations and phenotype-genotype correlations. Am. J. Med. Genet. 97, 147–152.

Amir, R.E., Van den Veyver, I.B., Wan, M., Tran, C.Q., Francke, U., Zoghbi, H.Y., 1999. Rett syndrome is caused by mutations in X-linked MECP2, encoding methyl-CpG-binding protein 2. Nat. Genet. 23, 185–188.

Avruch, J., 1998. Insulin signal transduction through protein kinase cascades. Mol. Cell. Biochem. 182, 31–48.

Bird, A., 2002. DNA methylation patterns and epigenetic memory. Genes Dev. 16, 6–21.

Bonni, A., Sun, Y., Nadal-Vicens, M., Bhatt, A., Frank, D.A., Rozovsky, I., Stahl, N., Yancopoulos, G.D., Greenberg, M.E., 1997. Regulation of gliogenesis in the central nervous system by the JAK-STAT signaling pathway. Science 278, 477–483.

Brami-Cherrier, K., Valjent, E., Herve, D., Darragh, J., Corvol, J.C., Pages, C., Arthur, S.J., Girault, J.A., Caboche, J., 2005. Parsing molecular and behavioral effects of cocaine in mitogen- and stress-activated protein kinase-1-deficient mice. J. Neurosci. 25, 11444–11454.

Cao, Q.L., Zhang, Y.P., Howard, R.M., Walters, W.M., Tsoulfas, P., Whittemore, S.R., 2001. Pluripotent stem cells engrafted into the normal or lesioned adult rat spinal cord are restricted to a glial lineage. Exp. Neurol. 167, 48–58.

Chahrour, M., Jung, S.Y., Shaw, C., Zhou, X., Wong, S.T., Qin, J., Zoghbi, H.Y., 2008. MeCP2, a key contributor to neurological disease, activates and represses transcription. Science 320, 1224–1229.

Chao, H.T., Zoghbi, H.Y., Rosenmund, C., 2007. MeCP2 controls excitatory synaptic strength by regulating glutamatergic synapse number. Neuron 56, 58–65.

Chen, R.Z., Akbarian, S., Tudor, M., Jaenisch, R., 2001. Deficiency of methyl-CpG binding protein-2 in CNS neurons results in a Rett-like phenotype in mice. Nat. Genet. 27, 327–331.

Chong, J.A., Tapia-Ramirez, J., Kim, S., Toledo-Aral, J.J., Zheng, Y., Boutros, M.C., Altshuller, Y.M., Frohman, M.A., Kraner, S.D., Mandel, G., 1995. REST: a mammalian silencer protein that restricts sodium channel gene expression to neurons. Cell 80, 949–957.

Colantuoni, C., Jeon, O.H., Hyder, K., Chenchik, A., Khimani, A.H., Narayanan, V., Hoffman, E.P., Kaufmann, W.E., Naidu, S., Pevsner, J., 2001. Gene expression profiling in postmortem Rett syndrome brain: differential gene expression and patient classification. Neurobiol. Dis. 8, 847–865.

Collins, A.L., Levenson, J.M., Vilaythong, A.P., Richman, R., Armstrong, D.L., Noebels, J.L., David Sweatt, J., Zoghbi, H.Y., 2004. Mild overexpression of MeCP2 causes a progressive neurological disorder in mice. Hum. Mol. Genet. 13, 2679–2689.

Conti, L., Pollard, S.M., Gorba, T., Reitano, E., Toselli, M., Biella, G., Sun, Y., Sanzone, S., Ying, Q.L., Cattaneo, E., Smith, A., 2005. Niche-independent symmetrical self-renewal of a mammalian tissue stem cell. PLoS Biol. 3, e283.

Edlund, T., Jessell, T.M., 1999. Progression from extrinsic to intrinsic signaling in cell fate specification: a view from the nervous system. Cell 96, 211–224.

Fan, G., Martinowich, K., Chin, M.H., He, F., Fouse, S.D., Hutnick, L., Hattori, D., Ge, W., Shen, Y., Wu, H., ten Hoeve, J., Shuai, K., Sun, Y.E., 2005. DNA methylation controls the timing of astrogliogenesis through regulation of JAK-STAT signaling. Development 132, 3345–3356.

Gage, F.H., 2000. Mammalian neural stem cells. Science 287, 1433–1438.

Gomes, W.A., Mehler, M.F., Kessler, J.A., 2003. Transgenic overexpression of BMP4 increases astroglial and decreases oligodendroglial lineage commitment. Dev. Biol. 255, 164–177.

Gross, R.E., Mehler, M.F., Mabie, P.C., Zang, Z., Santschi, L., Kessler, J.A., 1996. Bone morphogenetic proteins promote astroglial lineage commitment by mammalian subventricular zone progenitor cells. Neuron 17, 595–606.

Hofstetter, C.P., Holmstrom, N.A., Lilja, J.A., Schweinhardt, P., Hao, J., Spenger, C., Wiesenfeld-Hallin, Z., Kurpad, S.N., Frisen, J., Olson, L., 2005. Allodynia limits the usefulness of intraspinal neural stem cell grafts; directed differentiation improves outcome. Nat. Neurosci. 8, 346–353.

Hsieh, J., Gage, F.H., 2004. Epigenetic control of neural stem cell fate. Curr. Opin. Genet. Dev. 14, 461–469.

Johansson, C.B., Momma, S., Clarke, D.L., Risling, M., Lendahl, U., Frisen, J., 1999. Identification of a neural stem cell in the adult mammalian central nervous system. Cell 96, 25–34.

Jones, P.L., Veenstra, G.J., Wade, P.A., Vermaak, D., Kass, S.U., Landsberger, N., Strouboulis, J., Wolffe, A.P., 1998. Methylated DNA and MeCP2 recruit histone deacetylase to repress transcription. Nat. Genet. 19, 187–191.

Jung, B.P., Zhang, G., Ho, W., Francis, J., Eubanks, J.H., 2002. Transient forebrain ischemia alters the mRNA expression of methyl DNA-binding factors in the adult rat hippocampus. Neuroscience 115, 515–524.

Kishi, N., Macklis, J.D., 2004. MECP2 is progressively expressed in post-migratory neurons and is involved in neuronal maturation rather than cell fate decisions. Mol. Cell. Neurosci. 27, 306–321.

Klose, R.J., Bird, A.P., 2006. Genomic DNA methylation: the mark and its mediators. Trends Biochem. Sci. 31, 89–97.

Kohyama, J., Kojima, T., Takatsuka, E., Yamashita, T., Namiki, J., Hsieh, J., Gage, F.H., Namihira, M., Okano, H., Sawamoto, K., Nakashima, K., 2008. Epigenetic regulation of neural cell differentiation plasticity in the adult mammalian brain. Proc. Natl. Acad. Sci. U. S. A. 105, 18012–18017.

Kouhara, H., Hadari, Y.R., Spivak-Kroizman, T., Schilling, J., Bar-Sagi, D., Lax, I., Schlessinger, J., 1997. A lipid-anchored Grb2-binding protein that links FGF-receptor activation to the Ras/MAPK signaling pathway. Cell 89, 693–702.

Lim, D.A., Tramontin, A.D., Trevejo, J.M., Herrera, D.G., Garcia-Verdugo, J.M., Alvarez-Buylla, A., 2000. Noggin antagonizes BMP signaling to create a niche for adult neurogenesis. Neuron 28, 713–726.

Meehan, R.R., Lewis, J.D., Bird, A.P., 1992. Characterization of MeCP2, a vertebrate DNA binding protein with affinity for methylated DNA. Nucleic Acids Res. 20, 5085–5092.

Menard, C., Hein, P., Paquin, A., Savelson, A., Yang, X.M., Lederfein, D., Barnabe-Heider, F., Mir, A.A., Sterneck, E., Peterson, A.C., Johnson, P.F., Vinson, C., Miller, F.D., 2002. An essential role for a MEK-C/EBP pathway during growth factor-regulated cortical neurogenesis. Neuron 36, 597–610.

Morita, S., Kojima, T., Kitamura, T., 2000. Plat-E: an efficient and stable system for transient packaging of retroviruses. Gene. Ther. 7, 1063–1066.

Nakamura, M., Houghtling, R.A., MacArthur, L., Bayer, B.M., Bregman, B.S., 2003. Differences in cytokine gene expression profile between acute and secondary injury in adult rat spinal cord. Exp. Neurol. 184, 313–325.

Nakashima, K., Wiese, S., Yanagisawa, M., Arakawa, H., Kimura, N., Hisatsune, T., Yoshida, K., Kishimoto, T., Sendtner, M., Taga, T., 1999a. Developmental requirement of gp130 signaling in neuronal survival and astrocyte differentiation. J. Neurosci. 19, 5429–5434.

Nakashima, K., Yanagisawa, M., Arakawa, H., Kimura, N., Hisatsune, T., Kawabata, M., Miyazono, K., Taga, T., 1999b. Synergistic signaling in fetal brain by STAT3-Smad1 complex bridged by p300. Science 284, 479–482.

Nakashima, K., Takizawa, T., Ochiai, W., Yanagisawa, M., Hisatsune, T., Nakafuku, M., Miyazono, K., Kishimoto, T., Kageyama, R., Taga, T., 2001. BMP2-mediated alteration in the developmental pathway of fetal mouse brain cells from neurogenesis to astrocytogenesis. Proc. Natl. Acad. Sci. U. S. A. 98, 5868–5873.

Namihira, M., Nakashima, K., Taga, T., 2004. Developmental stage dependent regulation of DNA methylation and chromatin modification in a immature astrocyte specific gene promoter. FEBS Lett. 572, 184–188.

Namihira, M., Kohyama, J., Semi, K., Sanosaka, T., Deneen, B., Taga, T., Nakashima, K., 2009. Committed neuronal precursors confer astrocytic potential on residual neural precursor cells. Dev. Cell. 16, 245–255.

Namiki, J., Tator, C.H., 1999. Cell proliferation and nestin expression in the ependyma of the adult rat spinal cord after injury. J. Neuropathol. Exp. Neurol. 58, 489–498.

Nan, X., Ng, H.H., Johnson, C.A., Laherty, C.D., Turner, B.M., Eisenman, R.N., Bird, A., 1998. Transcriptional repression by the methyl-CpG-binding protein MeCP2 involves a histone deacetylase complex. Nature 393, 386–389.

Ogawa, Y., Sawamoto, K., Miyata, T., Miyao, S., Watanabe, M., Nakamura, M., Bregman, B.S., Koike, M., Uchiyama, Y., Toyama, Y., Okano, H., 2002. Transplantation of in vitro-expanded fetal neural progenitor cells results in neurogenesis and functional recovery after spinal cord contusion injury in adult rats. J. Neurosci. Res. 69, 925–933.

Paquin, A., Barnabe-Heider, F., Kageyama, R., Miller, F.D., 2005. CCAAT/enhancer-binding protein phosphorylation biases cortical precursors to generate neurons rather than astrocytes in vivo. J. Neurosci. 25, 10747–10758.

Pollard, S.M., Conti, L., Sun, Y., Goffredo, D., Smith, A., 2006. Adherent neural stem (NS) cells from fetal and adult forebrain. Cereb. Cortex 16 (Suppl. 1), i112–i120.

Qian, X., Shen, Q., Goderie, S.K., He, W., Capela, A., Davis, A.A., Temple, S., 2000. Timing of CNS cell generation: a programmed sequence of neuron and glial cell production from isolated murine cortical stem cells. Neuron 28, 69–80.

Rajan, P., McKay, R.D., 1998. Multiple routes to astrocytic differentiation in the CNS. J. Neurosci. 18, 3620–3629.

Schoenherr, C.J., Anderson, D.J., 1995. The neuron-restrictive silencer factor (NRSF): a coordinate repressor of multiple neuron-specific genes. Science 267, 1360–1363.

Setoguchi, T., Nakashima, K., Takizawa, T., Yanagisawa, M., Ochiai, W., Okabe, M., Yone, K., Komiya, S., Taga, T., 2004. Treatment of spinal cord injury by transplantation of fetal neural precursor cells engineered to express BMP inhibitor. Exp. Neurol. 189, 33–44.

Setoguchi, H., Namihira, M., Kohyama, J., Asano, H., Sanosaka, T., Nakashima, K., 2006. Methyl-CpG binding proteins are involved in restricting differentiation plasticity in neurons. J. Neurosci. Res. 84, 969–979.

Shahbazian, M.D., Antalffy, B., Armstrong, D.L., Zoghbi, H.Y., 2002. Insight into Rett syndrome: MeCP2 levels display tissue- and cell-specific differences and correlate with neuronal maturation. Hum. Mol. Genet. 11, 115–124.

Stancheva, I., Collins, A.L., Van den Veyver, I.B., Zoghbi, H., Meehan, R.R., 2003. A mutant form of MeCP2 protein associated with human Rett syndrome cannot be displaced from methylated DNA by notch in *Xenopus* embryos. Mol. Cell. 12, 425–435.

Sun, Y., Nadal-Vicens, M., Misono, S., Lin, M.Z., Zubiaga, A., Hua, X., Fan, G., Greenberg, M. E., 2001. Neurogenin promotes neurogenesis and inhibits glial differentiation by independent mechanisms. Cell 104, 365–376.

Takizawa, T., Nakashima, K., Namihira, M., Ochiai, W., Uemura, A., Yanagisawa, M., Fujita, N., Nakao, M., Taga, T., 2001. DNA methylation is a critical cell-intrinsic determinant of astrocyte differentiation in the fetal brain. Dev. Cell. 1, 749–758.

Vroemen, M., Aigner, L., Winkler, J., Weidner, N., 2003. Adult neural progenitor cell grafts survive after acute spinal cord injury and integrate along axonal pathways. Eur. J. Neurosci. 18, 743–751.

Zhou, Z., Hong, E.J., Cohen, S., Zhao, W.N., Ho, H.Y., Schmidt, L., Chen, W.G., Lin, Y., Savner, E., Griffith, E.C., Hu, L., Steen, J.A., Weitz, C.J., Greenberg, M.E., 2006. Brain-specific phosphorylation of MeCP2 regulates activity-dependent Bdnf transcription, dendritic growth, and spine maturation. Neuron 52, 255–269.

Roles of Sema4D–Plexin-B1 Interactions in the Central Nervous System for Pathogenesis of Experimental Autoimmune Encephalomyelitis

Tatsusada Okuno,*,†,‡ Yuji Nakatsuji,‡ Masayuki Moriya,‡ Hyota Takamatsu,*,† Satoshi Nojima,*,† Noriko Takegahara,*,† Toshihiko Toyofuku,*,† Yukinobu Nakagawa,*,† Sujin Kang,*,† Roland H. Friedel,§,1 Saburo Sakoda,‡ Hitoshi Kikutani,¶ and Atsushi Kumanogoh*,†

Although semaphorins were originally identified as axonal guidance molecules during neuronal development, it is emerging that several semaphorins play crucial roles in various phases of immune responses. Sema4D/CD100, a class IV semaphorin, has been shown to be involved in the nervous and immune systems through its receptors plexin-B1 and CD72, respectively. However, the involvement of Sema4D in neuroinflammation still remains unclear. We found that Sema4D promoted inducible NO synthase expression by primary mouse microglia, the effects of which were abolished in plexin-B1–deficient but not in CD72-deficient microglia. In addition, during the development of experimental autoimmune encephalomyelitis (EAE), which was induced by immunization with myelin oligodendrocyte glycoprotein-derived peptides, we observed that the expression of Sema4D and plexin-B1 was induced in infiltrating mononuclear cells and microglia, respectively. Consistent with these expression profiles, when myelin oligodendrocyte glycoprotein-specific T cells derived from wild-type mice were adoptively transferred into plexin-B1–deficient mice or bone marrow chimera mice with plexin-B1–deficient CNS resident cells, the development of EAE was considerably attenuated. Furthermore, blocking Abs against Sema4D significantly inhibited neuroinflammation during EAE development. Collectively, our findings demonstrate the role of Sema4D–plexin-B1 interactions in the activation of microglia and provide their pathologic significance in neuroinflammation. ***The Journal of Immunology*****, 2010, 184: 1499–1506.**

Microglia, resident immune effector cells in the CNS, are thought to play a key role in the regulation of neuroinflammation (1). Although activated microglia are known to exert a beneficial role in host defense and tissue repair in the CNS, it has been suggested that they also participate in propagation of inflammation in the CNS through Ag presentation, production of proinflammatory cytokines or chemokines, and NO (2–4). In fact, the mechanisms of how activation of microglia is regulated have been extensively studied. For example, CD40, a member of the TNF receptor family, has been reported to be involved in microglial activation (5, 6). Interactions of CD40 with its ligand (CD154), which is primarily expressed by activated T cells, promote the activation of microglia in the context of enhanced expression of costimulatory molecules and production of proinflammatory cytokines or chemokines and NO (5). Therefore, CD40–CD40 ligand interactions have been implicated in various neurologic disorders such as multiple sclerosis, Alzheimer's disease, and Parkinson's disease (5, 7, 8). However, answers are elusive regarding how the immunoregulatory molecules are involved in neuroinflammation.

Sema4D/CD100 is a transmembrane-type semaphorin belonging to the class IV semaphorin subclass. Although semaphorins were initially identified as axonal guidance cues during neuronal development (9, 10), accumulating evidence now indicates that several semaphorins play a crucial role in physiologic and pathologic immune responses (11). The expression of Sema4D is abundantly observed in T cells, but only weakly detected in naive B cells, macrophages, and dendritic cells (DCs); however, its expression is significantly upregulated on cellular activation (12, 13). Regarding its receptor systems, Sema4D has been shown to use two distinct receptors, plexin-B1 in the nervous system and CD72 in the immune system (11, 14, 15). We previously demonstrated the activation of B cells and DCs through the Sema4D–CD72 interactions (15, 16); Sema4D-deficient mice display severe impairments in activation of B cells and DCs, resulting in impaired Ab production and Ag-specific T cell priming (13, 16). In the nervous system, Sema4D participates in axon guidance by regulating activities of RhoA

*Department of Immunopathology, ¶Department of Molecular Immunology, Research Institute for Microbial Diseases, †World Premier International Immunology Frontier Research Center, and ‡Department of Neurology, Osaka University Graduate School of Medicine, Osaka University, Osaka, Japan; and §Institute of Developmental Genetics, Helmholtz Center Munich, Neuherberg, Germany

[1]Current address: Department of Developmental and Regenerative Biology, Mount Sinai School of Medicine, New York, NY.

Received for publication October 13, 2009. Accepted for publication November 14, 2009.

This work was supported by research grants from the Ministry of Education, Culture, Sports, Science and Technology of Japan; Health and Labour Sciences Research Grants for research on intractable diseases from the Ministry of Health, Labor, and Welfare; the program for Promotion of Fundamental Studies in Health Sciences of the National Institute of Biomedical Innovation (to A.K., Y.N., and S.S.); the Target Protein Research Program of the Japan Science and Technology Agency (to T.T. and A.K.); the Uehara Memorial Foundation (to A.K.); and the Takeda Scientific Foundation (to T.T. and A.K.).

Address correspondence and reprint requests to Atsushi Kumanogoh, Department of Immunopathology, Research Institute for Microbial Diseases, Osaka University, 3-1 Yamada-oka, Suita, Osaka 565-0871, Japan, or Yuji Nakatsuji, Department of Neurology (D4), Osaka University Graduate School of Medicine, 2-2 Yamada-oka, Suita, Osaka 565-0871, Japan. E-mail addresses: kumanogo@ragtime.biken.osaka-u.ac.jp or yuji@neurol.med.osaka-u.ac.jp

The online version of this article contains supplemental material.

Abbreviations used in this paper: BM, bone marrow; DC, dendritic cell; EAE, experimental autoimmune encephalomyelitis; iNOS, inducible NO synthase; MG, primary microglia; MOG, myelin oligodendrocyte glycoprotein; PLP, proteolipid protein; SB, SB203580; SP, SP600125; St, standards.

www.jimmunol.org/cgi/doi/10.4049/jimmunol.0903302

through PDZ-ρ guanine nucleotide exchange factors and leukemia-associated RhoGEF (17). In addition, plexin-B1 has been shown to mediate repellent signals in hypocampal neurons by directly binding Rnd1 and downregulating R-ras activity in response to Sema4D (18). Collectively, these findings indicate the importance of Sema4D in both nervous and immune systems.

Regarding neuroinflammation, in which the immune system interacts with the nervous system, it has been suggested that semaphorins are pathogenetically significant. Sema7A expressed in T cells regulates inflammation of experimental autoimmune encephalomyelitis (EAE) (19, 20). In addition, it has been reported that Sema4D is relevant to HTLV-1–associated myelopathy (21). The expression of Sema4D was increased in the cerebrospinal fluid and spinal cords of patients with HTLV-1–associated myelopathy, in which T cell-derived Sema4D impaired immature oligodendrocytes (21). In addition, we previously reported that Sema4D-deficient mice were resistant to the development of EAE because of the impaired Ag-specific T cell priming in the draining lymph nodes (16). Although these facts suggest the relevance of Sema4D in neuroinflammatory diseases, it has not been fully elucidated how and to what extent Sema4D is involved in neuroinflammation.

In this study, we demonstrate enhanced activation of microglia through Sema4D–plexin-B1 interactions. In addition, we find that either plexin-B1–deficient mice or bone marrow (BM) chimera mice with CNS-specific plexin-B1 deficiency were resistant to the development of EAE after adoptive transfer of myelin oligodendrocyte glycoprotein (MOG)-specific T cells. We further present that the treatment with an Ab against Sema4D was effective for EAE blocking, including in the effector phase. These findings demonstrate the significance of Sema4D–plexin-B1 interactions in the inflamed CNS and provide a novel therapeutic target for neuroinflammatory diseases.

Materials and Methods

Mice

Sema4D- and plexin-B1–deficient on the C57BL/6 background were generated and maintained as described previously (13, 22, 23). CD72-deficient mice were provided by Dr. Parnes (Stanford University, Stanford, CA) (24). C57BL/6 (CD45.2 and CD45.1) and SJL mice were purchased from Nippon Clea (Hamamatsu, Japan) and Nippon Charles River (Kanagawa, Japan), respectively. All mice used in this study were maintained in a specific pathogen-free environment. All animal experimental procedures were consistent with our institutional guidelines.

Reagents for cell cultures

Agonistic anti-CD40 Ab (HM40-3), and recombinant mouse interferon-γ (IFN-γ) were purchased from BD Biosciences (San Diego, CA), and Genzyme-Techne (Cambridge, MA), respectively. Recombinant Sema4D, consisting of the extracellular region of Sema4D and the Fc portion of human IgG1 (Sema4D-Fc), was made as previously described (16). Human IgG, p38 MAPK inhibitor SB203580, MEK inhibitor U0126, and JNK inhibitor SP600125 were purchased from Calbiochem (San Diego, CA).

Cell cultures and immunocytochemistry

Microglial cell line GMI-6-3 (6-3 cells) were grown in MEM (Sigma-Aldrich, St Louis, MO) containing 10% FBS, 0.2% glucose, and 5 μg/ml bovine insulin. Primary microglia were prepared as described (8, 25). Mixed cells prepared from cerebrums of newborn mice were cultured in media (10% FBS-DMEM) for 14 d. Next, microglia were detached by shaking, and the detached cells were replated onto a noncoated dish. After 30 min incubation at 37°C, adherent cells were scraped, centrifuged, and replated onto poly-L-lysine–coated 35-mm dishes (for Western blotting, 2×10^5 cells/cm^2) or eight-well Lab-Tec chamber slides (for immunostaining, 1×10^4 cells/cm^2; for measurement of nitrite, 5×10^5 cells/cm^2).

For inducible NO synthase (iNOS), CD72, or plexin-B1 staining, microglia were fixed with 4% paraformaldehyde for 15 min. After blocking with 2% BSA (Sigma-Aldrich) in PBS containing Fc-block (1:20, anti-CD16/32, 2.4G2; BD Biosciences) for 30 min, cells were incubated with rabbit anti-iNOS (1:100; BD Biosciences), mouse anti-CD72 (1:100; BD Biosciences) or mouse anti–plexin-B1 (1:50; Santa Cruz Biotechnology, Santa Cruz, CA) Abs at 4°C overnight, followed by staining with FITC-conjugated goat anti-rabbit or mouse IgG Ab (1:300, Cappel, West Chester, PA). For microglial-staining, PE-conjugated rat anti-CD11b Ab (1:100; BD Biosciences) was used. Images were collected using a confocal microscope (Carl Zeiss) equipped with IMARIS software.

Measurement of nitrite

NO production by activated microglia was determined by measuring the amounts of nitrite, a stable oxidation product of NO using Griess reactions in triplicates. An aliquot of the conditioned medium was mixed with an equal volume of 1% sulfanilamide in water and 0.1% N-1-naphthylethylenediamine dihydrochloride in 5% phosphoric acid. The absorbance was determined at 550 nm. Statistical significance was analyzed using an unpaired Student t test, and $p \leq 0.05$ was considered significant.

Western blot analysis

Western blot analysis was performed as previously described (26). Cell lysates were lysed with radio-immunoprecipitation assay buffer (PBS, 1% NP-40, 0.5% sodium deoxycholate, 0.1% SDS, pH7.4) containing protease inhibitors (20 μg/ml aprotinin, 1 mM phenyl-methylsulfonyl fluoride) and 1 mM sodium orthovanadate. The same amounts of total proteins were

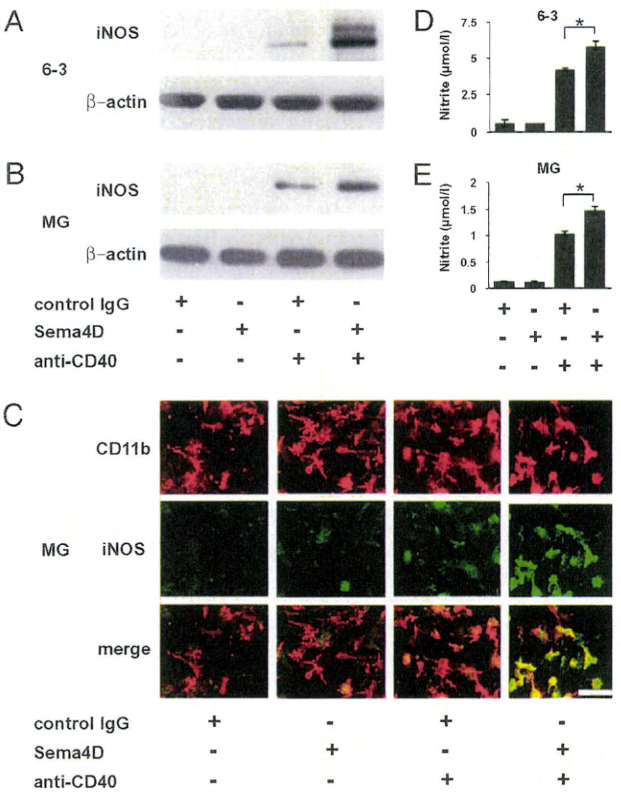

FIGURE 1. Sema4D enhances iNOS expression and NO production in microglial cells. *A* and *B*, Western blots for the iNOS expression in microglia revealed the enhancement of iNOS expression by Sema4D in a microglial cell line (6-3) (*A*) and primary microglia (MG) (*B*). INOS expression was strongly upregulated by incubation with recombinant Sema4D-Fc proteins. β-Actin was used as an internal control for Western blot analysis. *C*, Immunocytochemical analysis for iNOS expression in primary MG. The number of iNOS-positive microglia was markedly enhanced by Sema4D-Fc. CD11b was used as a microglial marker. Scale bar, 20 μm. *D* and *E*, Measurement of nitrite concentrations in the culture supernatants from microglial cell line (6-3) (*D*) and MG (*E*). Nitrite production was significantly increased by addition of Sema4D-Fc in microglia. Data are shown as mean ± SEM of triplicate wells. $*p < 0.05$. MG or microglial cell line (6-3) were incubated with indicated reagents: human IgG (20 μg/ml), Sema4D-Fc (20 μg/ml), anti-CD40 (0.5 μg/ml), plus IFN-γ (5 U/ml) for 24 h (for Western blot analysis and immunocytochemistry) or 72 h (for measurement of nitrite concentrations). The data presented are representative of three independent experiments.

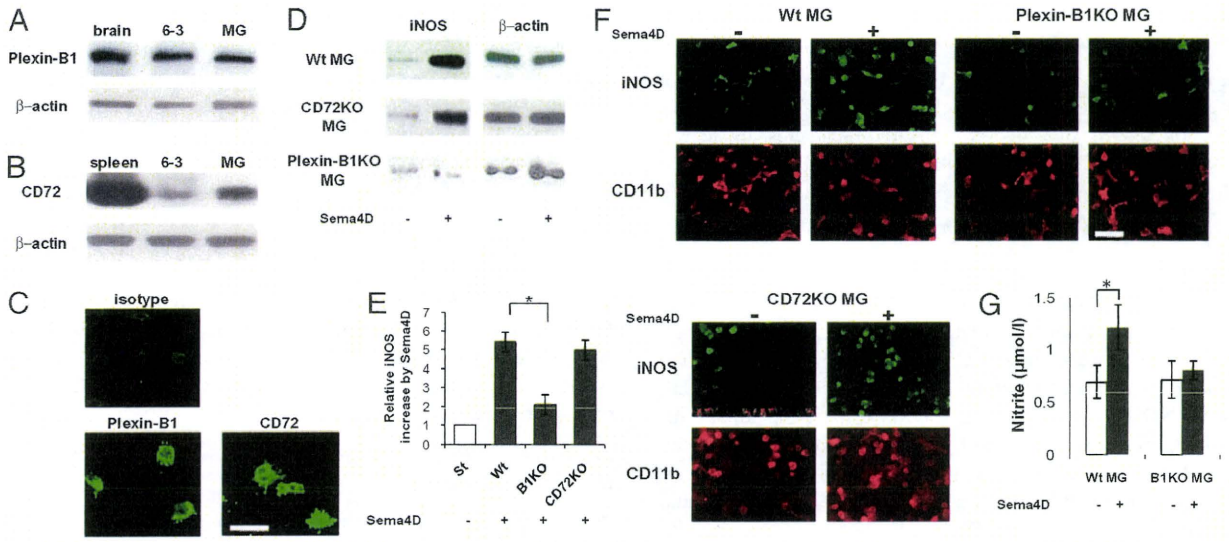

FIGURE 2. INOS and NO production by Sema4D is abolished in plexin-B1–deficient but not in CD72-deficient microglia. *A* and *B*, Western blot analysis for plexin-B1 (*A*) and CD72 (*B*) in microglia. Lysates of the brain or spleen (positive controls) were prepared. *C*, Immunocytochemical analysis for plexin-B1 and CD72 in microglial cell line (6-3). Both plexin-B1 and CD72 were expressed in microglia. Scale bar, 20 μm. *D*, Western blot analysis for iNOS expression. The induction of iNOS expression by addition of Sema4D-Fc was abolished in plexin-B1–deficient microglia, but markedly enhanced in either wild-type or CD72-deficient cells. β-Actin was used as an internal control. *E*, Relative iNOS increase by addition of Sema4D-Fc in microglia from wild-type, CD72-deficient, and plexin-B1–deficient mice. The levels of iNOS expression in microglia incubated with anti-CD40 and IFN-γ plus human IgG without Sema4D-Fc were defined as standards (St). Data are shown as mean ± SEM. $*p < 0.05$. *F*, Immunocytochemical analysis for iNOS expression in primary microglia. The number of microglia positive for iNOS was not increased by Sema4D-Fc in plexin-B1–deficient microglia, but increased in wild-type and CD72-deficient cells. Scale bar, 50 μm. *G*, Nitrite concentrations in the culture supernatants. The increase of nitrite production in the culture supernatants by addition of Sema4D-Fc was not observed in plexin-B1–deficient microglia. Data are shown as mean ± SEM of triplicate wells. $*p < 0.05$. For iNOS or NO production, cells were treated with (20 μg/ml) or without Sema4D-Fc in the presence of anti-CD40 (0.5 μg/ml) and IFN-γ (5 U/ml) for 24 h (for Western blot or immunocytochemical analysis) or 72 h (for measurement of nitrite concentrations). The data presented in are representative of at least three independent experiments.

resolved on 10% SDS-polyacrylamide gels, transferred to polyvinylidene difluoride membranes (Millipore, MA), and blotted with one of the following Abs at 4°C overnight: rabbit anti-CD72 (1:500, Santa Cruz Biotechnology), mouse anti–plexin-B1 (1:150, Santa Cruz Biotechnology), rabbit anti-iNOS (1:300, BD Biosciences), rabbit anti-phospho-ERK1/2 (1:300, Cell Signaling Technology, Danvers, MA), goat anti-MAPK (1:500, Santa Cruz Biotechnology), rabbit anti-total or phospho-JNK (Santa Cruz Biotechnology), rabbit anti-total or phospho-p38 (Santa Cruz Biotechnology) or mouse anti–β-actin (1:8000; Sigma-Aldrich) Abs. They were subsequently incubated with appropriate secondary Abs conjugated with HRP for 60 min and visualized by ECL reagents (Amersham Biosciences, Buckinghamshire, U.K.). The image of each band was captured and analyzed using Image Gauge (Fuji Film, Tokyo, Japan), which allows quantification of the bands. Statistical significance was analyzed using an unpaired Student *t* test; $p \leq 0.05$ was considered significant.

Establishment of BM chimeric mice

BM cells were isolated by flushing femur and tibia bones with HBSS. BM was filtered through a 100-μm cell strainer and cells were washed with HBSS. CD45.2 recipient mice were lethally irradiated with 950 cGy and injected i.v. with 2×10^6 CD45.1 BM cells. Engraftment took place over 6–8 wk of recovery. Mice were bled retro-orbitally to ensure 95% engraftment of blood leukocytes.

Induction of EAE

EAE was induced in 6- to 8-wk-old wild-type or plexin-B1–deficient mice on a C57BL/6 background following s.c. injection of 100 μg mouse/rat MOG_{35-55} peptides (MEVGWYRSPFSPVVHLYRNGK) emulsified in CFA, in addition to two i.v. injections of 100 ng pertussis toxin (List Laboratories, Campbell, CA) on days 0 and 2. Relapsing EAE was induced in 8-wk-old SJL mice by an s.c. immunization with 200 μl of a CFA containing 200 μg *Mycobacterium tuberculosis* H37Ra (Difco Laboratories, Sparks, MD) and 150 μg proteolipid protein $(PLP)_{139-151}$ (HSLGKWLGHPDKF) distributed over three sites on the lateral hind flanks and dorsally. All mice were monitored daily for clinical signs and were scored using a scale of 0–4 as follows: 0, no overt signs of diseases; 1, limp tail; 2, complete hind limb paralysis; 3, complete forelimb paralysis; 4, moribund state or death. Statistical significance was analyzed using an unpaired Student *t* test, and $p \leq 0.05$ was considered significant. For adoptive transfer, donor mice were immunized with MOG/CFA in the same fashion as except for no pertussis toxin. Ten days later, spleens and draining lymph nodes were collected, single-cell suspensions were prepared, and RBCs were lysed. Cells (5×10^6 cells/ml) were cultured with 40 μg/ml MOG_{35-55} peptide and 10 ng/ml recombinant mouse IL-12 (R&D Systems, Minneapolis, MN). After 3 d culture, cells were harvested and $CD4^+$ T cells were isolated by negative selection using Dynabeads (Invitrogen, Carlsbad, CA). Recipient mice irradiated sublethally (500 cGy) received cells i.v.

Immunohistochemistry

Mice were sacrificed followed by transcardiac perfusion with 4% paraformaldehyde in PBS. For Sema4D, plexin-B1, and iNOS labeling, sections (10 μm) were incubated with mouse anti–plexin-B1, mouse anti-Sema4D, or rabbit anti-iNOS Ab (1:50; Santa Cruz Biotechnology) at 4°C overnight, followed by biotin-conjugated secondary Abs (1:200, goat anti-rabbit or mouse; Vector Laboratories, Burlington, CA) for 30 min, then stained with PE-conjugated streptavidin. For double labeling, rabbit anti-IBA-1 Ab (for microglia/macrophage, 1:500; Wako, Osaka, Japan), FITC-conjugated anti-CD3 Ab (for T cells, 1:500; BD Pharmingen), and rabbit anti-GFAP Ab (for astrocytes, 1:1000; DakoCytomation, Carpinteria, CA) were used. Images were collected using a confocal microscope (Carl Zeiss, Oberkochen, Germany) equipped with IMARIS software (Bitplane AG, Zurich, Switzerland).

Mononuclear cell isolation from CNS and flow cytometry

Mice were euthanized with injection of pentobarbital, and spinal cords and brains were dissected. Both tissues were homogenized and strained through a 70-μm nylon filter (Falcon, Franklin Lakes, NJ). After centrifugation, the cell suspension was resuspended in 37% isotonic Percoll (GE Healthcare, Uppsala, Sweden) and underlayed with 70% isotonic Percoll. The gradient was centrifuged at $600 \times g$ for 25 min at room temperature. The interphase cells were collected and extensively washed before staining. For flow cytometry, the cells were stained with biotinylated anti-Sema4D, FITC-conjugated anti-CD3, APC-conjugated CD11b mAbs for 30 min at 4°C, washed, and incubated with streptavidin-PE (BD Pharmingen. San Diego, CA) for 15 min. The cells were washed and analyzed using a FACS Canto-2 using Diva software (BD Biosciences). Postacquisition analysis was performed using Flow Jo (Tomy Digital Biology, Tokyo, Japan).

Results

Sema4D enhances iNOS and NO production in microglia

To investigate the involvement of Sema4D in activation of microglia, we first examined the effects of Sema4D on the production of iNOS, one of the effector molecules in neuroinflammation (8, 27). Although iNOS production by a microglial cell line 6-3 cells or primary microglia was not detected upon incubation with recombinant Sema4D or control IgG alone (Fig. 1*A*, 1*B*), Sema4D enhanced iNOS production in the presence of anti-CD40 agonistic Ab (Fig. 1*A*, 1*B*). Similar findings were obtained using immunocytochemical analysis, such that iNOS staining was significantly upregulated by the stimulation with Sema4D in the presence of anti-CD40 agonistic Ab (Fig. 1*C*). We then examined NO production by microglia to determine whether iNOS, an NO-synthesizing isoenzyme, is responsible for the increased NO production induced by Sema4D. Consistent with the effects of Sema4D on iNOS expression, the concentrations of nitrite were considerably increased by Sema4D in both 6-3 cells and primary microglia (Fig. 1*D*, 1*E*). Collectively, these results indicate that Sema4D has enhancing effects on CD40-mediated microglial activation.

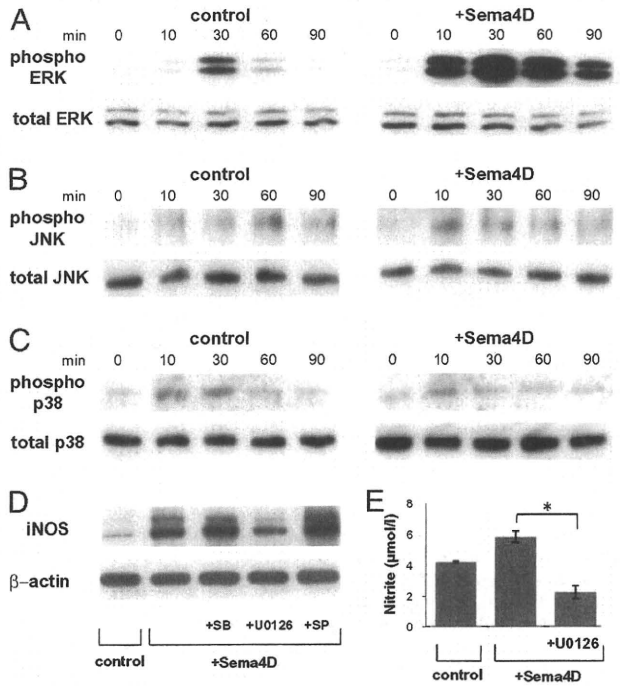

FIGURE 3. Sema4D enhances iNOS and NO production through ERK activation. *A–C*, Activation of ERK1/2, JNK, and p38 in 6-3 microglia stimulated with (*right panel*) or without (*left panel*) Sema4D-Fc. The same amounts of protein extracted from cultured cells incubated with human IgG (20 μg/ml) or Sema4D-Fc (20 μg/ml) for the indicated time in the presence of suboptimal doses of anti-CD40 plus IFN-γ were subjected to immunoblot analysis using Abs against phospho-ERK1/2 (*A*), total ERK1/2 (*A*), phospho-JNK (*B*), total JNK (*B*), phospho-p38 (*C*), and p38 (*C*). *D*, Effects of MAPK inhibitors on iNOS expression in Sema4D-treated 6-3 microglia. Cells were stimulated with Sema4D-Fc in the presence or absence of indicated kinase inhibitors for 24 h (SB203580 [SB]; p38 inhibitor, U0126; MEK1/2 inhibitor, SP600125 [SP]; JNK inhibitor). β-Actin was used as an internal control. *E*, The effect of U0126 on nitrite production from Sema4D-treated 6-3 microglia. Cells were treated with or without U0126 in the presence of suboptimal doses of anti-CD40 and IFN-γ plus Sema4D for 24 h. Data are shown as mean ± SEM of triplicate wells. $*p < 0.05$. The data are representative of three independent experiments.

Sema4D-induced iNOS and NO production is mediated through plexin-B1

Because Sema4D uses two receptors, plexin-B1 and CD72 (11), we examined their expression in microglia. As shown in Fig. 2*A–C*, the expression of plexin-B1 and CD72 proteins was observed in microglia. To address the question of which receptor is responsible for Sema4D-dependent microglial activation, we prepared microglia from plexin-B1– or CD72–deficient mice and examined their responses to Sema4D. Interestingly, the activating effects of Sema4D on microglia were significantly abolished in plexin-B1–deficient but not in CD72-deficient cells (Fig. 2*D–F*). Consistent with this, Sema4D-dependent NO production was also abolished in plexin-B1–deficient microglia (Fig. 2*G*). Collectively, these results strongly suggest that the stimulatory activities of Sema4D on microglia are mediated through plexin-B1.

Activation of ERK1/2 is responsible for Sema4D-mediated iNOS upregulation

Previous reports have shown that activation of ERK1/2 plays a key role in iNOS expression in microglia (28). In addition, the activation of other members of MAPK family, JNK and p38, is also shown to be involved in iNOS induction in glial cells (28, 29). We sought to determine whether Sema4D stimulation has an influence on ERK1/2, JNK, and p38 activation in microglia. Following stimulation with anti-CD40 agonistic Ab, phosphorylation of each kinase was observed within 10 min and then gradually declined within 90 min. Sema4D strongly enhanced ERK1/2 phosphorylation, moderately enhanced JNK phosphorylation at 10 min, and sustained ERK1/2 phosphorylation even at 90 min (Fig. 3*A*, 3*B*). However, apparent enhancement of p38 phosphorylation was not observed by the incubation with Sema4D (Fig. 3*C*).

We next examined whether the activation of these kinases induced by Sema4D was relevant to iNOS induction using several kinase inhibitors. Neither SP600125, a JNK inhibitor nor SB203580, a p38 inhibitor, did not inhibit the iNOS-upregulation by Sema4D. However, U0126, an MEK1 inhibitor, displayed an inhibitory effect on Sema4D-induced iNOS and NO production (Fig. 3*D*, 3*E*). These results suggest that enhanced activation of ERK1/2 is involved in Sema4D-mediated microglial activation.

Sema4D–plexin-B1 interactions in the CNS are involved in the pathogenesis of EAE

The in vitro findings suggest that Sema4D–plexin-B1 interactions are crucially involved in microglial activation. To address the role of Sema4D–plexin-B1 interactions during in vivo pathologic neuroinflammation, we examined the expression of Sema4D and plexin-B1 in pathogenic lesions of EAE. Although the expression of Sema4D was hardly seen in the spinal cords of control mice, it was significantly induced in infiltrating mononuclear cells of the spinal cords of mice with EAE (Fig 4*A*, 4*B*). To determine which cells expressed Sema4D in the CNS, we performed a double immunolabeling and found that $CD3^+$ T cells and a part of IBA-1^+ microglia/macrophage populations expressed Sema4D ($CD3^+$ T cells; 41 ± 2.1%, IBA-1^+ cells; 25 ± 4.1%, respectively; Fig. 4*C*, 4*D*). To further evaluate the expression of Sema4D on the surface of infiltrating mononuclear cells, we prepared mononuclear cell suspension from the brains and spinal cords of mice with EAE and analyzed them by flow cytometry. Consistent with the immunohistochemical analysis, $CD11b^+$ microglia/macrophage and $CD3^+$ T cells in the CNS of mice with EAE expressed Sema4D, whereas those from control mice did not (Fig. 4*E*, 4*F*).

Regarding plexin-B1, its expression was significantly increased in the lesions of mice with EAE, but not detected in the spinal cords of control mice (Fig. 5*A*, 5*B*). Notably, large populations of

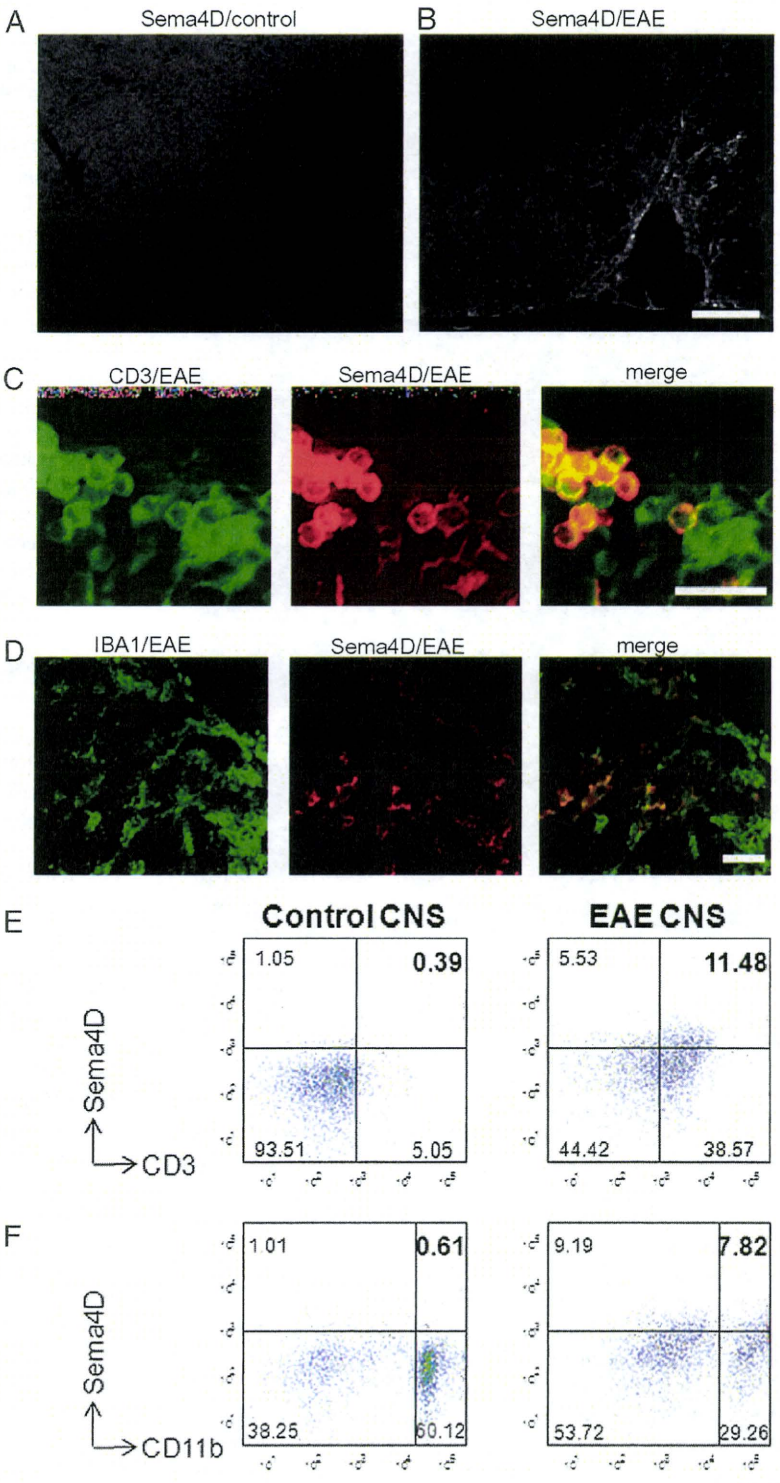

FIGURE 4. Expression of Sema4D is induced in EAE. *A* and *B*, Immunostaining of the spinal cords of control or mice with EAE. Sema4D-positive cells were not seen in the control spinal cords (*A*). By contrast, Sema4D-positive cells were abundantly observed in the white matter of EAE (*B*). Scale bar, 200 μm. *C*, A large population of CD3-positive cells were also positive for Sema4D. Scale bar, 50 μm. *D*, IBA-1–positive cells were also positive for Sema4D in mice with EAE. *E* and *F*, FACS analysis for the expression of Sema4D on $CD3^+$ or $CD11b^+$ cells in the CNS. Mononuclear cells derived from spinal cords and brains were separated by discontinuous Percoll gradient and stained with anti-Sema4D, anti-CD3, and anti-CD11b mAbs. Sema4D-positive $CD3^+$ cells or $CD11b^+$ cells were increased in the CNS of mice with EAE. EAE was induced by immunization of C57BL/6 mice with MOG_{35-55} peptides. Expression of Sema4D in the CNS was determined 7 d after the clinical onset. Age-matched nontreated mice were used as controls. Scale bar, 50 μm. All data presented are representative of analyses of three control mice with EAE.

IBA-1–positive microglia/macrophage were positive for plexin-B1 in the lesions of mice with EAE (Fig. 5*C*), whereas only a small part of CD3- or GFAP-positive cells expressed plexin-B1 (Fig. 5*D*, 5*E*). However, the expression of CD72 was not detected in the spinal cords of mice with EAE (data not shown).

We previously reported that Sema4D-deficient mice fail to develop EAE because of impaired T cell priming in the draining lymph nodes (Supplemental Fig. 1) (16). However, it has not been clarified how and to what extent Sema4D–plexin-B1 interactions in the CNS are pathologically significant during the course of EAE development. The fact that the expression of both Sema4D and plexin-B1 was induced in the lesions of EAE (Figs. 4 and 5) led us to investigate the pathologic importance of Sema4D–plexin-B1 interactions in the CNS during the course of EAE.

When we induced EAE by immunizing wild-type or plexin-B1–deficient mice with MOG_{35-55} peptides, together with pertussis toxin and CFA, plexin-B1–deficient mice displayed a relatively attenuated disease course and delayed clinical onset (Fig. 6*A*). To exclude a possibility that plexin-B1 is involved in T cell priming in the peripheral lymphoid organs, we examined the Ag-specific

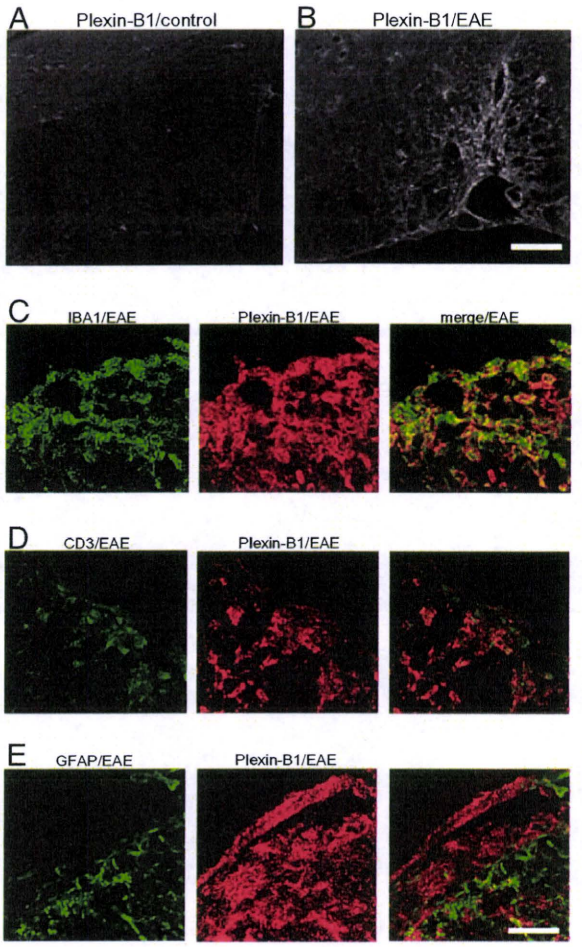

FIGURE 5. Expression of plexin-B1 is induced in EAE. *A* and *B*, Immunostaining of the spinal cords of control or mice with EAE. Plexin-B1-positive cells were not seen in the control white matter. In contrast, more plexin-B1–positive cells were observed in the white matter of EAE lesions. Scale bar, 200 μm. *C*, Most of IBA-1-positive cells were positive for plexin-B1. *D*, A small population of CD3-positive cells was positive for plexin-B1, and a large population of plexin-B1-positive cells was CD3-negative. *E*, A few GFAP-positive cells expressed plexin-B1. Scale bar, 50 μm. All data presented are representative of analyses of three control mice with EAE.

T cell priming in the draining lymph nodes in plexin-B1–deficient mice. Neither proliferation nor cytokine production in response to Ag were affected in plexin-B1–deficient mice (Supplemental Fig. 2), indicating that Sema4D–plexin-B1 interactions outside the CNS are not responsible for the resistance of EAE.

Next, to determine the pathogenic interactions between Sema4D and plexin-B1in the CNS, we adoptively transferred wild-type, MOG-specific T cells to wild-type or plexin-B1–deficient recipient mice. As is the case for active immunization, plexin-B1–deficient recipient mice displayed a diminished disease course and delayed clinical onset, compared with wild-type recipient mice (Fig. 6*B*). Consistent with the clinical course of EAE, an infiltration of mononuclear cells in the spinal cord of plexin-B1–deficient recipient mice was markedly attenuated (Fig. 6*C*). Furthermore, the expression of iNOS in the spinal cords was significantly reduced in plexin-B1–deficient recipient mice (Fig. 6*D*). To more extensively evaluate the involvement of plexin-B1 in the CNS during EAE-development, we generated BM chimera mice by transplanting wild-type CD45.1 BM cells to CD45.2 plexin-B1–deficient or wild-type mice (Wt→plexin-B1 KO, Wt→Wt), and adoptively transferred wild-type MOG-specific T cells to these chimera mice. As observed in active immunization of plexin-B1–deficient mice with MOG_{35-55} peptides, the lack of plexin-B1 expression in CNS resident cells caused a less severe disease course and delayed onset, compared with chimeric mice that express plexin-B1 in CNS resident cells (Fig. 6*E*).

Sema4D could be detected on IBA-1–positive cells in the spinal cords of mice with EAE (Fig. 4). To exclude a possible contribution of Sema4D expression in non-T cells, we adoptively transferred MOG-specific T cells into wild-type or Sema4D-deficient recipients. As shown in Fig. 6*F*, Sema4D-deficient recipient mice showed severities of EAE comparable to those observed in wild-type recipient mice, indicating that Sema4D expressed in non-T cells is not critical in the progression of EAE. Furthermore, blocking Abs against Sema4D considerably inhibited the development of relapsing EAE induced by an immunization with proteolipid protein $PLP_{139-151}$ peptides, including when they were administered after priming phases (Fig. 6*G*). Consistent with the clinical course of EAE, an infiltration of mononuclear cells in the spinal cords of mice treated with anti-Sema4D Abs was markedly attenuated (Fig. 6*H*). Collectively, these findings strongly support the notion that Sema4D–plexin-B1 interactions in the CNS are pathologically involved in the development of EAE.

Discussion

Sema4D activates microglia through plexin-B1

Activation of microglia has been shown to play a crucial role in inflammation-mediated neurologic disorders, such as multiple sclerosis and Alzheimer's disease, by producing various kinds of inflammatory effector molecules. In this study, we demonstrate that Sema4D activates microglia by increasing NO production via a plexin-B1–dependent mechanism. Further, T cell-derived Sema4D is crucially involved in the progression of EAE through interactions with plexin-B1 expressed in microglia.

In the immune system, we previously reported that Sema4D enhances CD40 signaling in B cells and DCs (15, 16). Consistent with these previous findings, we found that Sema4D promoted CD40-mediated activation of microglial cells. However, the mechanisms seem to be different between immune cells and microglia. Sema4D is known to use two types of receptors, plexin-B1 in the nervous system and CD72 in the immune system. plexin-B1 mediates Sema4D-induced axon guidance in the CNS (18), and CD72 mediates Sema4D-dependent modulation of the CD40 pathway in peripheral immune responses (15, 30). Despite the expression of CD72 on microglia, the enhancement of iNOS expression was still observed in CD72-deficient microglia. In contrast, the effects of Sema4D were significantly abolished in plexin-B1–deficient microglia (Fig. 2). These results indicate that enhancement of iNOS expression in microglia by Sema4D occurs in a CD72-independent and plexin-B1–dependent manner. It has been demonstrated that plexin-B1 displays higher affinity to Sema4D than CD72 (31). It thus appears that Sema4D preferentially binds to plexin-B1 in microglia because of its higher affinity to Sema4D rather than CD72 (31).

NO production by Sema4D is mediated via ERK pathways

An activation of MAPK family members, such as ERK and p38, has been shown to play a critical role in the regulation of iNOS and TNF-α in microglia (28, 32). It has been reported that CD40 stimulation in microglia results in an activation of Ras-MAPK pathway via phosphorylaion of Src family proteins Lck and Lyn, leading to the production of proinflammatory cytokines such as TNF-α (33). Similarly, Sema4D was reported to activate Ras-MAPK pathway downstream of plexin-B1 in neuronal cells and endothelial cells

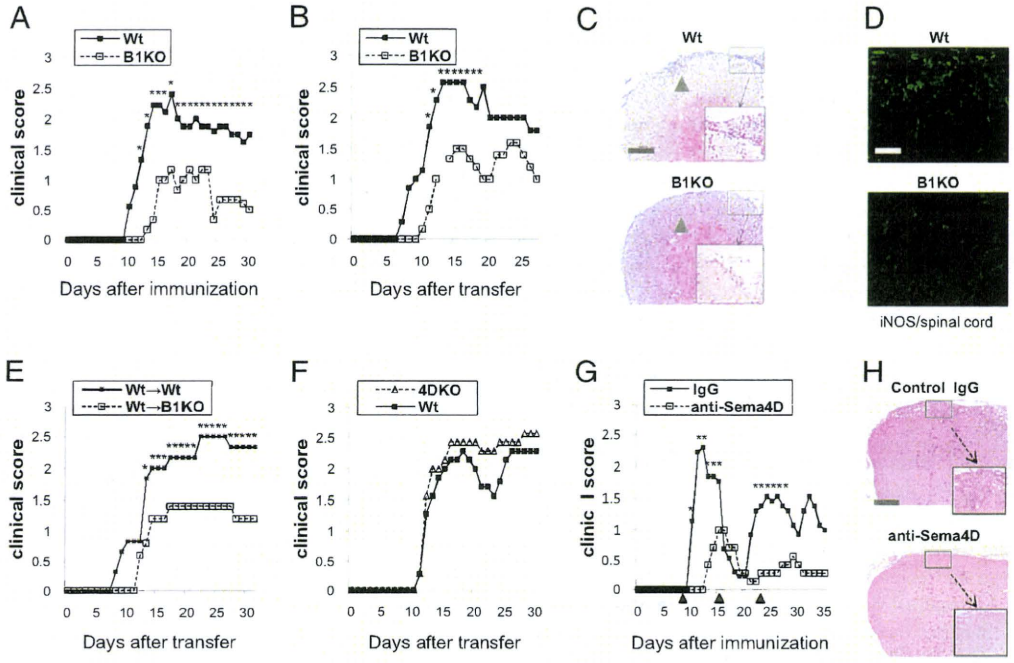

FIGURE 6. Plexin-B1–deficient mice exhibit reduced susceptibility to EAE due to the attenuated neuroinflammation. *A*, Clinical course of actively immunized EAE in plexin-B1–deficient mice. Wild-type ($n = 7$, closed squares) and plexin-B1–deficient ($n = 7$, open squares) mice were immunized with 100 μg MOG_{35-55} peptides in CFA; 100 ng of pertussis toxin was injected i.v. on days 0 and 2. The mean clinical score was calculated by averaging the scores of the mice in each group. $*p < 0.05$. *B*, Adoptive transfer of MOG-specific T cells into plexin-B1–deficient recipients induced attenuated EAE, compared with transfer into wild-type recipients. MOG-specific T cells were adoptively transferred into sublethally irradiated recipients (wild-type recipients, $n = 7$; plexin-B1–deficient recipients, $n = 8$). $*p < 0.05$. *C*, Spinal cord sections (7 d after the clinical onset) stained with H&E. The spinal cords of plexin-B1–deficient recipients had less infiltration of inflammatory mononuclear cells. Infiltrating mononuclear cells are indicated with arrowheads. The boxed areas show higher magnification. Scale bar, 300 μm. *D*, Spinal cord sections (7 d after the clinical onset) stained with anti-iNOS Ab. Reduced iNOS expression was observed in the spinal cords of plexin-B1–deficient recipients. Scale bar, 50 μm. *E*, Adoptive transfer of MOG-specific T cells into wild-type→plexin-B1–deficient BM chimeras resulted in less severe EAE, compared with transfer into wild-type→wild-type mice. BM chimeras were generated by transplanting wild-type BM cells to lethally irradiated plexin-B1–deficient or wild-type mice. Ten weeks after transplantation, MOG-specific T cells were adoptively transferred into sublethally irradiated recipients (wild-type→plexin-B1–deficient mice, $n = 6$; wild-type→wild-type mice, $n = 6$). $*p < 0.05$. *F*, Adoptive transfer of MOG-specific T cells into Sema4D-deficient recipients induced EAE similar to that induced in wild-type recipients (wild-type recipients, $n = 7$; Sema4D-deficient recipients, $n = 7$). *G*, Anti-Sema4D blocking Abs inhibited clinical progression of relapsing EAE. SJL mice were primed with $PLP_{139-151}$/CFA as described in *Materials and Methods*. Mice were treated with either anti-Sema4D (clones 5H7 and 3E9, $n = 7$) or control IgG ($n = 12$) on days 9, 16, and 23 (arrowheads). $*p < 0.05$. *H*, Spinal cord sections from relapsing EAE (30 d after the immunization) stained with H&E. The spinal cords of mice treated with anti-Sema4D Abs had less infiltration of inflammatory mononuclear cells than with control IgG. The boxed areas show higher magnification. Scale bar, 300 μm. The data presented in *A*, *B*, and *E–G* are representative of at least two independent experiments. Data presented in *C*, *D*, and *H* are representative of analyses of at least three mice in each group.

(34, 35). These findings prompted us to investigate the activation of MAPK family members, and this study provides evidence that the phosphorylation of ERK was significantly enhanced by Sema4D in concert with CD40 (Fig. 3). Furthermore, the enhancement of iNOS expression by Sema4D was inhibited by an inhibitor of ERK, but not by inhibitors of p38 or JNK (Fig. 3). These results support a role of ERK activation in the regulation of iNOS production by Sema4D in microglia. It has been reported that plexin-B1, through association with PDZ-ρ guanine nucleotide exchange factors and leukemia-associated RhoGEF, is involved in activation of RhoA in response to Sema4D (17, 36) and that ERK1/2 can be activated via plexin-B1 in neural cells and endothelial cells (34, 35). In this context, it is plausible that plexin-B1 regulates ERK1/2 signaling pathways in concert with CD40 signals. Further studies would be required to clarify the signaling mechanisms.

Interactions between Sema4D and plexin-B1 in the CNS are crucial for the progression of EAE

Consistent with our in vitro data that Sema4D–plexin-B1 interactions were involved in activation of microglia (Figs. 1 and 2), we further found that plexin-B1–deficient mice or BM chimera mice with a deficiency in plexin-B1 expression in the CNS were resistant to the development of EAE after an adoptive transfer of MOG-specific T cells (Fig. 6). It is well known that Sema4D is abundantly expressed on T cells (12). Indeed, in the pathologic lesions of EAE, Sema4D was expressed in infiltrating T cells in the spinal cords (Fig. 4), whereas plexin-B1 was expressed in microglia (Fig. 5). It thus appears that CNS- infiltrating, Sema4D-positive T cells can interact with plexin-B1–positive, CNS-resident microglia, resulting in activation of microglia during EAE progression. It is possible that BM-derived macrophages have some contribution to the neuroinflammation in EAE, because Sema4D is also expressed on cells other than T cells, such as IBA-1–positive microglia/macrophages in the spinal cords of mice with EAE (Fig. 4). However, there were not significant differences in the severity of EAE between Sema4D-deficient and wild-type recipient mice when transferred with wild-type MOG-specific T cells. This finding implies that T cell-derived Sema4D is primarily responsible for the pathogenesis of EAE through interactions with plexin-B1–expressing microglia. It is also possible that T cell-derived Sema4D has some influence on other CNS cells such as oligodendrocytes. In fact, Giraudon et al. (21) reported that T cell-derived Sema4D induces collapse of

process extension in immature oligodendrocytes and death of immature neural cells, resulting in compromised remyelination in the inflamed brain. However, plexin-B1–deficient mice displayed delayed onsets and decreased severities of EAE even at the early phase, which is difficult to explain simply with improved remyelination at the later phase of EAE. In addition, major populations of plexin-B1–positive cells were also positive for IBA-1, but negative for the oligodendrocyte marker OLIG-1 (data not shown). Collectively, these findings support the conclusion that attenuated development of EAE in plexin-B1–deficient mice is primarily due to impaired Sema4D-mediated microglial activation. However, we cannot completely exclude a possibility that Sema4D may directly injure oligodendrocytes in EAE. In addition, a possible protective effect of Sema4D in neuroinjury was recently suggested (37), although our experimental system could not reproduce such results.

In conclusion, we demonstrat that Sema4D–plexin-B1 interactions are crucially involved in activation of microglia. We also present that Sema4D is expressed in infiltrating T cells in the spinal cord of mice with EAE, whereas plexin-B1 is expressed in microglia and participates in the pathogenesis of EAE in the CNS. Furthermore, blocking Abs against Sema4D significantly inhibits neuroinflammation during EAE development. Together with our previous data that MOG-specific T cell priming is impaired in Sema4D-deficient mice (16), a blockade of Sema4D would be a valuable therapeutic target for neuroinflammatory diseases including EAE, because it can prevent the generation of encephalitogenic T cells and ameliorate inflammation even after clinical onset.

Acknowledgments

We thank T. Yazawa for technical support.

Disclosures

The authors have no financial conflicts of interests.

References

1. Ransohoff, R. M., and V. H. Perry. 2009. Microglial physiology: unique stimuli, specialized responses. *Annu. Rev. Immunol.* 27: 119–145.
2. Heppner, F. L., M. Greter, D. Marino, J. Falsig, G. Raivich, N. Hövelmeyer, A. Waisman, T. Rülicke, M. Prinz, J. Priller, et al. 2005. Experimental autoimmune encephalomyelitis repressed by microglial paralysis. *Nat. Med.* 11: 146–152.
3. Jack, C., F. Ruffini, A. Bar-Or, and J. P. Antel. 2005. Microglia and multiple sclerosis. *J. Neurosci. Res.* 81: 363–373.
4. Ponomarev, E. D., L. P. Shriver, and B. N. Dittel. 2006. CD40 expression by microglial cells is required for their completion of a two-step activation process during central nervous system autoimmune inflammation. *J. Immunol.* 176: 1402–1410.
5. Tan, J., T. Town, D. Paris, T. Mori, Z. Suo, F. Crawford, M. P. Mattson, R. A. Flavell, and M. Mullan. 1999. Microglial activation resulting from CD40-CD40L interaction after β-amyloid stimulation. *Science* 286: 2352–2355.
6. Becher, B., B. G. Durell, A. V. Miga, W. F. Hickey, and R. J. Noelle. 2001. The clinical course of experimental autoimmune encephalomyelitis and inflammation is controlled by the expression of CD40 within the central nervous system. *J. Exp. Med.* 193: 967–974.
7. Gerritse, K., J. D. Laman, R. J. Noelle, A. Aruffo, J. A. Ledbetter, W. J. Boersma, and E. Claassen. 1996. CD40-CD40 ligand interactions in experimental allergic encephalomyelitis and multiple sclerosis. *Proc. Natl. Acad. Sci. U.S.A.* 93: 2499–2504.
8. Okuno, T., Y. Nakatsuji, A. Kumanogoh, M. Moriya, H. Ichinose, H. Sumi, H. Fujimura, H. Kikutani, and S. Sakoda. 2005. Loss of dopaminergic neurons by the induction of inducible nitric oxide synthase and cyclooxygenase-2 via CD 40: relevance to Parkinson's disease. *J. Neurosci. Res.* 81: 874–882.
9. Kolodkin, A. L., D. J. Matthes, and C. S. Goodman. 1993. The semaphorin genes encode a family of transmembrane and secreted growth cone guidance molecules. *Cell* 75: 1389–1399.
10. Zhou, Y., R. A. Gunput, and R. J. Pasterkamp. 2008. Semaphorin signaling: progress made and promises ahead. *Trends Biochem. Sci.* 33: 161–170.
11. Suzuki, K., A. Kumanogoh, and H. Kikutani. 2008. Semaphorins and their receptors in immune cell interactions. *Nat. Immunol.* 9: 17–23.
12. Bougeret, C., I. G. Mansur, H. Dastot, M. Schmid, G. Mahouy, A. Bensussan, and L. Boumsell. 1992. Increased surface expression of a newly identified 150-kDa dimer early after human T lymphocyte activation. *J. Immunol.* 148: 318–323.
13. Shi, W., A. Kumanogoh, C. Watanabe, J. Uchida, X. Wang, T. Yasui, K. Yukawa, M. Ikawa, M. Okabe, J. R. Parnes, et al. 2000. The class IV semaphorin CD100 plays nonredundant roles in the immune system: defective B and T cell activation in CD100-deficient mice. *Immunity* 13: 633–642.
14. Tamagnone, L., S. Artigiani, H. Chen, Z. He, G. I. Ming, H. Song, A. Chedotal, M. L. Winberg, C. S. Goodman, M. Poo, et al. 1999. Plexins are a large family of receptors for transmembrane, secreted, and GPI-anchored semaphorins in vertebrates. *Cell* 99: 71–80.
15. Kumanogoh, A., C. Watanabe, I. Lee, X. Wang, W. Shi, H. Araki, H. Hirata, K. Iwahori, J. Uchida, T. Yasui, et al. 2000. Identification of CD72 as a lymphocyte receptor for the class IV semaphorin CD100: a novel mechanism for regulating B cell signaling. *Immunity* 13: 621–631.
16. Kumanogoh, A., K. Suzuki, E. Ch'ng, C. Watanabe, S. Marukawa, N. Takegahara, I. Ishida, T. Sato, S. Habu, K. Yoshida, et al. 2002. Requirement for the lymphocyte semaphorin, CD100, in the induction of antigen-specific T cells and the maturation of dendritic cells. *J. Immunol.* 169: 1175–1181.
17. Swiercz, J. M., R. Kuner, J. Behrens, and S. Offermanns. 2002. Plexin-B1 directly interacts with PDZ-RhoGEF/LARG to regulate RhoA and growth cone morphology. *Neuron* 35: 51–63.
18. Oinuma, I., Y. Ishikawa, H. Katoh, and M. Negishi. 2004. The Semaphorin 4D receptor Plexin-B1 is a GTPase activating protein for R-Ras. *Science* 305: 862–865.
19. Czopik, A. K., M. S. Bynoe, N. Palm, C. S. Raine, and R. Medzhitov. 2006. Semaphorin 7A is a negative regulator of T cell responses. *Immunity* 24: 591–600.
20. Suzuki, K., T. Okuno, M. Yamamoto, R. J. Pasterkamp, N. Takegahara, H. Takamatsu, T. Kitao, J. Takagi, P. D. Rennert, A. L. Kolodkin, et al. 2007. Semaphorin 7A initiates T-cell-mediated inflammatory responses through alpha1beta1 integrin. *Nature* 446: 680–684.
21. Giraudon, P., P. Vincent, C. Vuaillat, O. Verlaeten, L. Cartier, A. Marie-Cardine, M. Mutin, A. Bensussan, M. F. Belin, and L. Boumsell. 2004. Semaphorin CD100 from activated T lymphocytes induces process extension collapse in oligodendrocytes and death of immature neural cells. *J. Immunol.* 172: 1246–1255.
22. Friedel, R. H., G. Kerjan, H. Rayburn, U. Schüller, C. Sotelo, M. Tessier-Lavigne, and A. Chédotal. 2007. Plexin-B2 controls the development of cerebellar granule cells. *J. Neurosci.* 27: 3921–3932.
23. Friedel, R. H., A. Plump, X. Lu, K. Spilker, C. Jolicoeur, K. Wong, T. R. Venkatesh, A. Yaron, M. Hynes, B. Chen, et al. 2005. Gene targeting using a promoterless gene trap vector ("targeted trapping") is an efficient method to mutate a large fraction of genes. *Proc. Natl. Acad. Sci. USA* 102: 13188–13193.
24. Pan, C., N. Baumgarth, and J. R. Parnes. 1999. CD72-deficient mice reveal nonredundant roles of CD72 in B cell development and activation. *Immunity* 11: 495–506.
25. Kanzawa, T., M. Sawada, K. Kato, K. Yamamoto, H. Mori, and R. Tanaka. 2000. Differentiated regulation of allo-antigen presentation by different types of murine microglial cell lines. *J. Neurosci. Res.* 62: 383–388.
26. Okuno, T., Y. Nakatsuji, A. Kumanogoh, K. Koguchi, M. Moriya, H. Fujimura, H. Kikutani, and S. Sakoda. 2004. Induction of cyclooxygenase-2 in reactive glial cells by the CD40 pathway: relevance to amyotrophic lateral sclerosis. *J. Neurochem.* 91: 404–412.
27. Jana, M., X. Liu, S. Koka, S. Ghosh, T. M. Petro, and K. Pahan. 2001. Ligation of CD40 stimulates the induction of nitric-oxide synthase in microglial cells. *J. Biol. Chem.* 276: 44527–44533.
28. Bhat, N. R., P. Zhang, J. C. Lee, and E. L. Hogan. 1998. Extracellular signal-regulated kinase and p38 subgroups of mitogen-activated protein kinases regulate inducible nitric oxide synthase and tumor necrosis factor-α gene expression in endotoxin-stimulated primary glial cultures. *J. Neurosci.* 18: 1633–1641.
29. Han, I. O., K. W. Kim, J. H. Ryu, and W. K. Kim. 2002. p38 mitogen-activated protein kinase mediates lipopolysaccharide, not interferon-γ, -induced inducible nitric oxide synthase expression in mouse BV2 microglial cells. *Neurosci. Lett.* 325: 9–12.
30. Wang, X., A. Kumanogoh, C. Watanabe, W. Shi, K. Yoshida, and H. Kikutani. 2001. Functional soluble CD100/Sema4D released from activated lymphocytes: possible role in normal and pathologic immune responses. *Blood* 97: 3498–3504.
31. Kumanogoh, A., and H. Kikutani. 2001. The CD100-CD72 interaction: a novel mechanism of immune regulation. *Trends Immunol.* 22: 670–676.
32. Han, I. O., H. S. Kim, H. C. Kim, E. H. Joe, and W. K. Kim. 2003. Synergistic expression of inducible nitric oxide synthase by phorbol ester and interferon-γ is mediated through NF-kappaB and ERK in microglial cells. *J. Neurosci. Res.* 73: 659–669.
33. Tan, J., T. Town, M. Saxe, D. Paris, Y. Wu, and M. Mullan. 1999. Ligation of microglial CD40 results in p44/42 mitogen-activated protein kinase-dependent TNF-α production that is opposed by TGF-β 1 and IL-10. *J. Immunol.* 163: 6614–6621.
34. Aurandt, J., W. Li, and K. L. Guan. 2006. Semaphorin 4D activates the MAPK pathway downstream of plexin-B1. *Biochem. J.* 394: 459–464.
35. Basile, J. R., J. Gavard, and J. S. Gutkind. 2007. Plexin-B1 utilizes RhoA and ρ kinase to promote the integrin-dependent activation of Akt and ERK and endothelial cell motility. *J. Biol. Chem.* 282: 34888–34895.
36. Swiercz, J. M., R. Kuner, and S. Offermanns. 2004. Plexin-B1/RhoGEF-mediated RhoA activation involves the receptor tyrosine kinase ErbB-2. *J. Cell Biol.* 165: 869–880.
37. Toguchi, M., D. Gonzalez, S. Furukawa, and S. Inagaki. 2009. Involvement of Sema4D in the control of microglia activation. *Neurochem, Int.* 55: 573–580.

A midline switch of receptor processing regulates commissural axon guidance in vertebrates

Homaira Nawabi,[1,4] Anne Briançon-Marjollet,[1,4] Christopher Clark,[1] Isabelle Sanyas,[1] Hyota Takamatsu,[2] Tatsusada Okuno,[2] Atsushi Kumanogoh,[2] Muriel Bozon,[1] Kaori Takeshima,[3] Yutaka Yoshida,[3] Frédéric Moret,[1] Karima Abouzid,[1] and Valérie Castellani[1,5]

[1]University of Lyon, University of Lyon 1, Claude Bernard Lyon1, CGMC, UMR, CNRS 5534, F-69000 Lyon, France; [2]Department of Immunology, Research Institute for Microbial Diseases, Osaka University, Osaka, 565-0871, Japan; [3]Division of Developmental Biology, Cincinnati Children's Hospital Medical Center, Cincinnati, Ohio 45229, USA

Commissural axon guidance requires complex modulations of growth cone sensitivity to midline-derived cues, but underlying mechanisms in vertebrates remain largely unknown. By using combinations of ex vivo and in vivo approaches, we uncovered a molecular pathway controlling the gain of response to a midline repellent, Semaphorin3B (Sema3B). First, we provide evidence that Semaphorin3B/Plexin-A1 signaling participates in the guidance of commissural projections at the vertebrate ventral midline. Second, we show that, at the precrossing stage, commissural neurons synthesize the Neuropilin-2 and Plexin-A1 Semaphorin3B receptor subunits, but Plexin-A1 expression is prevented by a calpain1-mediated processing, resulting in silencing commissural responsiveness. Third, we report that, during floor plate (FP) in-growth, calpain1 activity is suppressed by local signals, allowing Plexin-A1 accumulation in the growth cone and sensitization to Sema3B. Finally, we show that the FP cue NrCAM mediates the switch of Plexin-A1 processing underlying growth cone sensitization to Sema3B. This reveals pathway-dependent modulation of guidance receptor processing as a novel mechanism for regulating guidance decisions at intermediate targets.

[*Keywords*: Axon guidance; midline crossing; semaphorin; calpain; commissural neurons]

Supplemental material is available at http://www.genesdev.org.

Received June 5, 2009; revised version accepted December 18, 2009.

The developing neuronal projections navigate along highly diverse environments and manage complex pathway choices to reach their specific target tissues. Axon trajectories are specified by multiple cues, and guidance decisions crucially depend on regulatory mechanisms controlling in time and space the expression, distribution, and activity of the guidance machinery, including ligands, receptors, and signaling effectors (Yu and Bargmann 2001). The pathfinding of long-distance projections proceeds in successive stages, with regularly positioned sources of attractants keeping axons in appropriate routes, referred to as intermediate targets. For example, in vertebrates, groups of neurons in the CNS send axon projections that navigate through a key intermediate target, the floor plate (FP), in which they cross the midline. In the developing spinal cord, commissural neurons reside in the dorsal horn, and their axons navigate ventromedially to cross the midline and turn rostrally, extending along longitudinal pathways. Axon tracts then contact various spinal and higher-center neurons to establish circuits participating in the left–right control of sensory modalities and motor behaviors (Colamarino and Tessier-Lavigne 1995). Extensive studies established that Netrins, Semaphorins, IgSFCAMs, Slits, and various morphogens combine contact and diffusible attractive and repulsive effects to control commissural axon pathfinding (Augsburger et al. 1999; Garbe and Bashaw 2004; Dickson and Gilestro 2006).

A key issue that long-distance projections have to solve is how to leave an intermediate target. One possibility is that, among the guidance cues to which they are exposed, commissural axons first perceive attractants, thus being guided toward the intermediate target, and second repellents during in-growth, thereby receiving instructions for intermediate target exit. Accordingly, spinal commissural axons are attracted to the FP by Netrins and Shh, but then lose their responsiveness to Netrins and become sensitive to midline-derived repellents of the Slit, Semaphorin, and Ephrin families (Kidd et al. 1998; Brose et al. 1999; Zou et al. 2000; Imondi and Kaprielian 2001). Very

[4]These authors contributed equally to this work.
[5]Corresponding author.
E-MAIL castellani@cgmc.univ-lyon1.fr; FAX 33-0472442685.
Article is online at http://www.genesdev.org/cgi/doi/10.1101/gad.542510.
Freely available online through the *Genes & Development* Open Access option.

little is known about the mechanisms through which these modulations are achieved. Suppression of Netrin attraction has been proposed to occur upon exposure to Slits, through the association of their respective DCC and Robo receptors (Stein and Tessier-Lavigne 2001). In flies, the sensitivity to Slits is silenced at the precrossing stage through a post-translational mechanism coupling the Slit receptor Robo to the Commissureless protein and targeting the complex for proteasomal degradation. This pathway is suppressed at the midline through a yet-unknown mechanism, thus enabling commissural axons to gain responsiveness to Slits (Keleman et al. 2002; Dickson and Gilestro 2006). However, the commissural-dependent mechanism has not proven effective in vertebrates, despite the conservation of Robo/Slit signaling at the ventral midline. Genetic approaches in mice indicated that a specific spliced variant of one of the three *Robo* genes, *robo3*, controls through a yet-unknown mechanism Robo1/2 signaling and responsiveness to Slits (Chen et al. 2008). Another key but yet-unsolved issue is whether acquisition of responsiveness to guidance cues results from experience-independent processes, with neurons being sensitized through an intrinsic mechanism, or rather from context-dependent pathways, with neurons being sensitized by signals localized at intermediate targets.

In this study, we explored the role of the midline repellent Semaphorin3B (Sema3B), a class 3 Semaphorin (Sema3) that was reported in in vitro assays to repel commissural axons after FP crossing (Zou et al. 2000). We show that crossing and post-crossing axon trajectories are defective in *Sema3B*-null embryos, consistent with a role for Sema3B in FP exit. We identify Plexin-A1 as the signaling coreceptor of Sema3B in this system, and show that *Plexin-A1*- and *Sema3B*-null embryos exhibit similar guidance defects of spinal commissural projections. We set up cultures of isolated FP tissue and dissociated commissural neurons and demonstrate that signals released by FP cells sensitize commissural growth cones to Sema3B. Naive commissural growth cones in culture and precrossing axon segments in vivo express the receptor subunit Nrp2, but Plexin-A1 level is very low. Upon exposure to FP signals conferring the response to Sema3B, Plexin-A1 level is up-regulated and the protein distributes in the peripheral growth cone structures. In spinal cord explant cultures, Plexin-A1 expression was detected in axons emerging after FP crossing, while it was very low in explants cultures in which the FP was removed. When electroporated in the chick neural tube, the fluorescence of a Plexin-A1-gfpPhLuo fusion, allowing visualizing of a cell surface protein pool, is turned on upon FP crossing, which demonstrates that a switch of Plexin-A1 level occurs in this intermediate target. Decreasing and increasing Plexin-A1 levels in cultured commissural neurons and in vivo is sufficient for altering growth cone responsiveness to Sema3B. Through various pharmacological and siRNA-based knockdown approaches, we show that the Plexin-A1 level is actively kept low at the precrossing stage due to the processing by calpain1, and that FP signals, by suppressing this protease pathway, enable accumulation of Plexin-A1 in commissural growth cones and sensitization to Sema3B. Consistently, calpain activity in unfixed embryonic spinal cord sections is detected in spinal neurons and precrossing axon segments, but not in crossing axon segments and FP cells. Pharmacological inhibition of calpain activity in vivo induces defects of FP in-growth and premature turning. Biochemical approaches demonstrated that this calpain activity directly processes Plexin-A1 at the precrossing stage. Last, we identify an active FP component, the Ig superfamily cell adhesion molecule NrCAM, in the switch of Plexin-A1 processing, triggering commissural axon sensitization to Sema3B.

Results

Sema3B/Plexin-A1 signaling is required for commissural axon guidance at the midline

We first examined *Sema3B* and *Nrp2* expression in embryonic day 11.5 (E11.5) and E12.5 developing mouse spinal cords by in situ hybridization. Consistent with previous work (Zou et al. 2000), *Sema3B* was found expressed at the ventral midline and in dorsal territories, while *Nrp2* mRNA was detected in the dorsal horn where commissural neurons reside (Fig. 1A; Supplemental Fig. S1A). These expression patterns were consistent with a role of Sema3B in the guidance of commissural projections. Next, we analyzed the trajectory of commissural axons in *Sema3B*-null mutant mice. Crossing and post-crossing commissural pathways were examined in spinal cord open book preparations by insertion of DiI (1,1′-dilinoleyl-3,3,3′,3′-tetramethylindocarbocyanine, 4-chlorobenzenesulfonate) crystals in the domain of commissural cell bodies (Fig. 1B). In contrast to axons that turned rostrally after midline crossing in the wild-type embryos in 80% of cases, axons from *Sema3B*-null embryos exhibited aberrant trajectories in 60% of cases, ranging from stalling or turning in the FP, caudal instead of rostral turning, and dorsally rather than ventrally directed growth after FP crossing (number of crystals/number of embryos: 72/19 for +/+, 47/12 for +/−, and 90/13 for −/−, from four litters) (Fig. 1C). In another set of experiments, we focused on FP-crossing phenotypes and compared the proportion of DiI-labeled tracts that could exit the FP (number of crystals/number of embryos: 52/six for +/+, 28/three for +/−, and 51/four for −/−, from two litters) (Fig. 1D). More than 60% exited the FP in the wild-type embryos for only 32% in the null embryos. Thus, the genetic ablation of *Sema3B* disrupts the behavior of crossing and post-crossing commissural axons. FP and interneuron markers were not modified by the loss of *Sema3B*, suggesting that these defects reflected a requirement for Sema3B guidance activity at the ventral midline (Supplemental Fig. S1B,C). The Sema3 signaling is mediated by Plexin-A family members that are obligatory Nrp coreceptors for the activation of transduction cascades (Kruger et al. 2005; Bechara et al. 2008). Until now, there was no information regarding the identity of the Plexin-A recruited to Nrp2 for mediating Sema3B effects in axon guidance. Based on expression patterns in in situ hybridization performed on E12.5 coronal sections, *Plexin-A1*

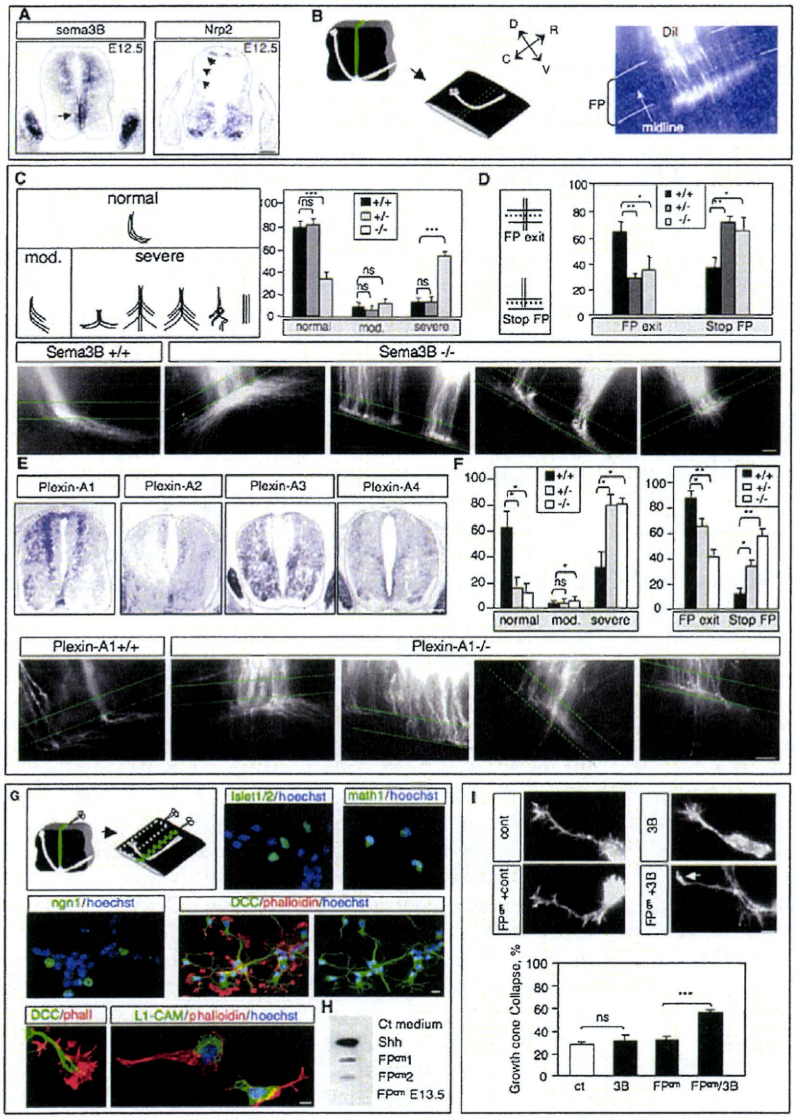

Figure 1. Crossing and post-crossing commissural defects in *Sema3B* and *Plexin-A1* knockout embryos, and gain of response to Sema3B induced by FP^{cm}. (*A*) In situ hybridization on E12.5 cross-sections showing *Sema3B* transcripts at the ventral midline and *Nrp2* in dorsal spinal cord domain of commissural neurons (arrows). (*B*) Schematic drawing of the spinal commissural pathway and DiI labeling in open book preparations. Green dashed lines delineate the FP positioned by phase-contrast observations. (*C*) Illustrations of commissural tracts in wild-type embryos (*Sema3B*$^{+/+}$) and various misrouting in the *Sema3B*-null embryos (*Sema3B* $^{-/-}$), stalling or turning in the FP, aberrant caudal turning, and dorsally directed growth. (*C*) Classification of commissural trajectories in normal, mild, and severe cases for *Sema3B*$^{+/+}$, *Sema3B*$^{+/-}$, and *Sema3B* $^{-/-}$ embryos. (*D*) Classification focused on axon behaviors within the FP showing that, at E12.5, significantly less axon tracts exited the FP in the +/− and −/− embryos than in the +/+ embryos. (*E*) In situ hybridization on E12.5 cross-sections to label *Plexin-A1*, *Plexin-A2*, *Plexin-A3*, and *Plexin-A4* transcripts in the spinal cord. *Plexin-A1* mRNA is strongly detected in spinal interneurons. (*F*) Illustrations and diagrams of DiI labeling of commissural projections in open book preparations from *Plexin-A1*$^{+/+}$ and *Plexin-A1* $^{-/-}$ embryos, showing aberrant crossing and post-crossing trajectories in the *Plexin-A1*-null embryos. Bars, 100 μm. (*G*) Schematic drawing of the tissue from which dissociated neuronal cultures and isolated FP tissue culture were performed. Cultured neurons express ngn1, math1, and islet 1/2 transcription factors, and cell surface DCC markers of commissural neurons. The L1-CAM marker is restricted to the soma in axon and growth cone compartment. (*H*) Slot blots showing immunodetection of the FP cue Shh in two FP^{cm} samples at E12.5 and its down-regulation at E13.5. (*I*) Histogram and microphotographs showing that FP^{cm} triggers a Sema3B-induced collapse response. Bar: *A*,*B*, 15 μm.

was the strongest candidate, as its transcript was detected in dorsal interneurons, while that of the other *Plexin-As* were not or were only weakly and/or uniformly distributed in the spinal cord (Fig. 1E; Cheng et al. 2001). We then examined spinal commissural projections in *Plexin-A1*-null embryos. DiIs were placed in open book preparations at stage E12.5/E13 (number of crystals/number of embryos: 54/six for +/+, 61/eight for +/−, and 84/seven for −/−, from five litters) (Fig. 1F). Errors of commissural axon trajectories were detected and, remarkably, they mimicked those identified in the *Sema3B*-null embryos, with premature turning, stalling in the FP, defasciculation, and caudal instead of rostral turning before and after crossing (Fig. 1F). FP and dorsal markers also were not affected by *Plexin-A1* genetic ablation (Supplemental Fig. S2A,B). This analysis supported that Plexin-A1 is required for Semaphorin3B-mediated axon guidance in the FP.

Local FP signals confer responsiveness to Sema3B

Explants assays established that commissural axons acquire responsiveness to Sema3B upon FP crossing (Zou et al. 2000). We confirmed this result in cocultures of open book explants with cell aggregates secreting Sema3B, observing that the growth of commissural axons toward cells secreting Sema3B was permitted when the FP was removed, but was inhibited in intact preparations

(five embryos, >15 explants/condition, three independent experiments) (Supplemental Fig. S3A). We hypothesized that the gain of response results from exposure to local signals present in the FP. To address this hypothesis, we set up cultures of isolated FP tissue to produce conditioned medium (FP^{cm}), and assessed it in a model of dissociated dorsal spinal neurons. To validate this model, we examined the expression of different commissural neuron markers (Fig. 1G). First, neurons composing the cultures expressed Islet1/2, math1, and ngn1 transcription factors characteristic of the dI1, dI2, and dI3 pools of commissural neurons. Second, the cell surface commissural marker DCC was detected in the axons and growth cones of all cultured neurons (Fig. 1G). In vivo, L1-CAM is expressed by commissural neurons, but is present only along crossing and post-crossing axon segments (Supplemental Fig. S3B). In our model, L1-CAM was detected in the soma and, strikingly, it was excluded in most cases from the axon and the growth cone compartments, and only occasionally $L1^+$ growth cones were detected (Fig. 1G; Supplemental Fig. S3B). Lastl initial axon outgrowth was dependent on netrin-1, as expected for commissural neurons (data not shown). Thus, cultured dissociated dorsal neurons express the markers of commissural neurons at the precrossing stage. To verify that the tissue put in culture was composed by FP cells, we assessed the presence of known soluble FP-derived cue Shh and Netrin-1 in slot blots, and could detect their presence in FP^{cm} samples (Fig. 1H; Supplemental Fig. S3C).

Next, the neuronal cultures were exposed to either control, Sema3B, or FP^{cm} treatment, or in combined application (Fig. 1I). Notably, the level of collapse was increased significantly by combined application of Sema3B and FP^{cm}, but not FP^{cm} or Sema3B alone (number of cones per condition/number of experiments: 560/seven for control, 560/seven for Sema3B, 1040/13 for FP^{cm}, and 1280/16 for FP^{cm}-Sema3B) (Fig. 1I). A similar gain of collapse was observed when the FP^{cm} was removed prior to Sema3B application, indicating that the FP^{cm} and Sema3B does not act in synergy, but rather that the FP^{cm} contains signals that capacitate commissural neurons to be responsive to Sema3B (Supplemental Fig. S3D). Commissural neurons isolated at E11.5, E12.5, and E13.5 all failed to collapse upon Sema3B exposure, indicating that neurons are unlikely to acquire responsiveness through maturation, at least in these culture conditions (Supplemental Fig. S3E).

Plexin-A1 level is up-regulated by FP signals in commissural growth cones

We hypothesized that responsiveness to Sema3B could be gained through regulation at the receptor complex level. Changes in expression levels, availability, or spatial distribution of some subunits could allow the growth cone to assemble a functional receptor only within the FP. To test this idea, we first examined the distribution of the receptor subunits in spinal commissural axons by immunohistochemistry on E11.5 cross-sections. The specificity of the anti-Plexin-A1 antibodies used for the study was controlled in transfected cells and in cross-sections of *Plexin-A1*-null embryos (Supplemental Fig. S4A,B). Nrp2 could be detected along both precrossing, crossing, and post-crossing axon shafts (Fig. 2A). Interestingly, Plexin-A1 expression was very weak in precrossing segments, but was strongly up-regulated in crossing and post-crossing segments (Fig. 2A). This raised first the possibility that commissural neurons are unresponsive to Sema3B due to the lack of Plexin-A1 in the growth cone, and second that Plexin-A1 expression and/or distribution could be modified during FP in-growth to allow commissural axons acquiring responsiveness to Sema3B. We thus investigated whether the FP^{cm} in our culture assay could regulate the expression of Plexin-A1. Interestingly, in the basal condition, Plexin-A1 was present in the central domain, but absent from the peripheral growth cone structures, playing key roles in the perception of extracellular signals. Remarkably, FP^{cm} application induced Plexin-A1 spreading in the growth cone filopodia (Fig. 2B). These observations were confirmed by counting of Plexin-A1 clusters (Fig. 2B). We found that the number of Plexin-A1 clusters increased by only 16% in the central domain, but by 160% in the filopodia. This was not due to morphological modifications, since the number of filopodia per growth cone was statistically comparable in all conditions (Fig. 2B). Thus, FP signals induce Plexin-A1 to accumulate in the filopodia.

We also asked whether the Plexin-A1 level is regulated by the FP^{cm} by performing quantitative fluorescence measurement, and found significant increase of the total Plexin-A1 pool in the soma and the growth cone (Fig. 2C,D). This result was confirmed with a second anti-Plexin-A1 antibody recognizing a different Plexin-A1 epitope (Supplemental Fig. S4A). A similar increase was also found when the quantitative analysis was restricted to the surface pool of Plexin-A1 (Fig. 2D). Such an increase was not observed for another Plexin-A family member, Plexin-A2 (Fig. 2E). Nrp2 was also not obviously modified after exposure to FP signals (Supplemental Fig. S5). We assessed the Plexin-A1 level with a complementary biochemical approach (Fig. 2F). Fresh dorsal spinal cord tissue was isolated for ex vivo stimulation by FP^{cm} and control treatments, and was processed for Western blot analysis. As expected, the Plexin-A1 level was increased by twofold in the FP^{cm} condition compared with the control, while the Nrp2 level remained comparable (Fig. 2F). To provide direct evidence that Plexin-A1 up-regulation takes place in axons that cross the FP, spinal cord explants in which the FP was either removed or left intact were cultured in a three-dimensional substrate and labeled with anti-DCC and anti-Plexin-A1 antibodies (Fig. 2G). Plexin-A1 and DCC levels were measured in growth cones that had or had not crossed the FP. We found that the DCC level remained constant in both conditions, while the Plexin-A1 level increased by 36% in growth cones that crossed the FP, thus demonstrating that axons must cross the FP to up-regulate Plexin-A1 (−FP, 64 growth cones; +FP, 34 growth cones; two independent experiments).

Next, we used the chick embryo to investigate the regulation of the Plexin-A1 level upon FP crossing in vivo. To validate this animal model for our question, we